The WRF NMM Core

Overview of Basic Principles

Zavisa Janjic
(Presented by Tom Black)

- Single digit resolutions becoming affordable for NWP, nonhydrostatic dynamics desirable

- What should a new nonhydrostatic NWP model be able to do?

  - Competitive with mature NWP models at transitional resolutions in accuracy and computational cost

  - Reproduce classical nonhydrostatic solutions at high resolutions

- WRF-NMM built on experiences of NWP
  - Relaxing the hydrostatic approximation, while,
  - Using modeling principles proven in NWP and regional climate applications
- Nonhydrostatic equations split into two parts
  - Hydrostatic part, except for higher order terms due to vertical acceleration
  - The part that allows computation of the corrections in the first part

- No linearizations or additional approximations required, fully compressible system
- The nonhydrostatic effects as an add–on nonhydrostatic module
  - Easy comparison of hydrostatic and nonhydrostatic solutions
  - Reduced computational effort at lower resolutions

- Pressure based vertical coordinate.
  - Exact mass (etc.) conservation
  - Nondivergent flow on pressure surfaces (often forgotten)
  - No problems with weak static stability
- "Competitive with mature hydrostatic NWP models" satisfied automatically with such an evolutionary approach?

➢Mass (hydrostatic pressure) based vertical coordinate

$$hydrostatic\ pressure = \frac{weight\ of\ the\ air\ in\ the\ column}{horizontal\ cross\ section\ of\ the\ column}$$

$$\rho = \frac{p}{RT};\ \alpha = \frac{1}{\rho} = \frac{RT}{p};\ p\ (nonhydrostatic)\ pressure$$

$$\Delta M = \rho \Delta S \Delta z$$

$$\frac{g \Delta M}{\Delta S} = \rho g \Delta z$$

$$\Delta \pi = \rho \Delta \Phi;\ \pi\ hydrostatic\ pressure$$

$$\frac{\Delta \Phi}{\Delta \pi} = \frac{1}{\rho} = \alpha$$

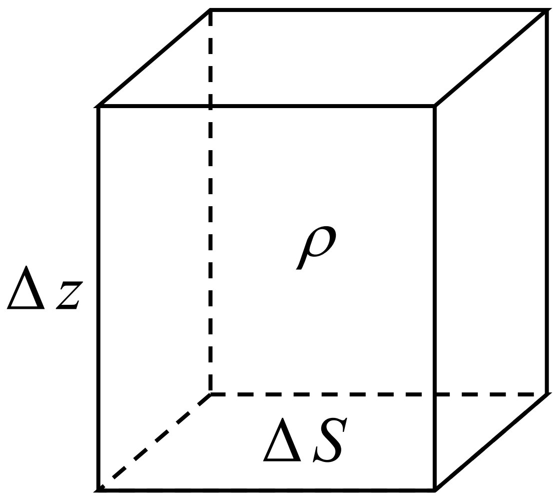

Hypsometric (not hydrostatic) equation

➢ Inviscid, adiabatic, sigma (Janjic et al., 2001):

$$\sigma = (\pi - \pi_t)/(\pi_s - \pi_t) \qquad \mu = \pi_s - \pi_t \qquad \varepsilon \equiv \frac{1}{g}\frac{dw}{dt}$$

$$\frac{d\mathbf{v}}{dt} = -(1+\varepsilon)\nabla_\sigma \Phi - \alpha \nabla_\sigma p + f\mathbf{k}\times\mathbf{v}$$

$$\frac{\partial T}{\partial t} = -\mathbf{v}\bullet\nabla_\sigma T - \dot{\sigma}\frac{\partial T}{\partial \sigma} + \frac{\alpha}{c_p}[\frac{\partial p}{\partial t} + \mathbf{v}\bullet\nabla_\sigma p + \dot{\sigma}\frac{\partial p}{\partial \sigma}]$$

$$\frac{\partial \mu}{\partial t} + \nabla_\sigma \bullet(\mu\mathbf{v}) + \frac{\partial(\mu\dot{\sigma})}{\partial \sigma} = 0$$

$$\alpha = RT/p$$

$$\frac{\partial \Phi}{\partial \sigma} = -\mu\frac{RT}{p}$$

Hydrostatic system, except for p and ε, $\frac{\partial p}{\partial \pi} = 1 + \varepsilon$

“Additional part”

$$\left(\frac{\partial T}{\partial t}\right)_2 = \frac{1}{c_p}\alpha\omega_2$$

$$\frac{\partial p}{\partial \pi} = 1 + \varepsilon$$ Third (vertical) Eq of motion

$$\frac{\partial \Phi}{\partial \sigma} = -\mu \frac{RT}{p}$$

$$w = \frac{1}{g}\frac{d\Phi}{dt} = \frac{1}{g}\left(\frac{\partial \Phi}{\partial t} + \mathbf{v} \bullet \nabla_\sigma \Phi + \dot{\sigma}\frac{\partial \Phi}{\partial \sigma}\right)$$ Nonhydrostatic cont. Eq

$$\varepsilon = \frac{1}{g}\frac{dw}{dt} = \frac{1}{g}\left(\frac{\partial w}{\partial t} + \mathbf{v} \bullet \nabla_\sigma w + \dot{\sigma}\frac{\partial w}{\partial \sigma}\right)$$

- Φ, w, ε not independent, no independent prognostic Eq for w!

- ε <<1 in meso and large scale atmospheric flows

- Impact of nonhydrostatic dynamics becomes detectable at resolutions <10km, important at 1km.

➢ Boundary conditions

- $\dot{\sigma} = 0$ top
- $\dot{\sigma} = 0$ bottom

➢ Additional

- $p - \pi = 0$ top
- $\dfrac{\partial(p - \pi)}{\partial\sigma} = 0$ bottom

➢ Rotated latitude-longitude coordinate

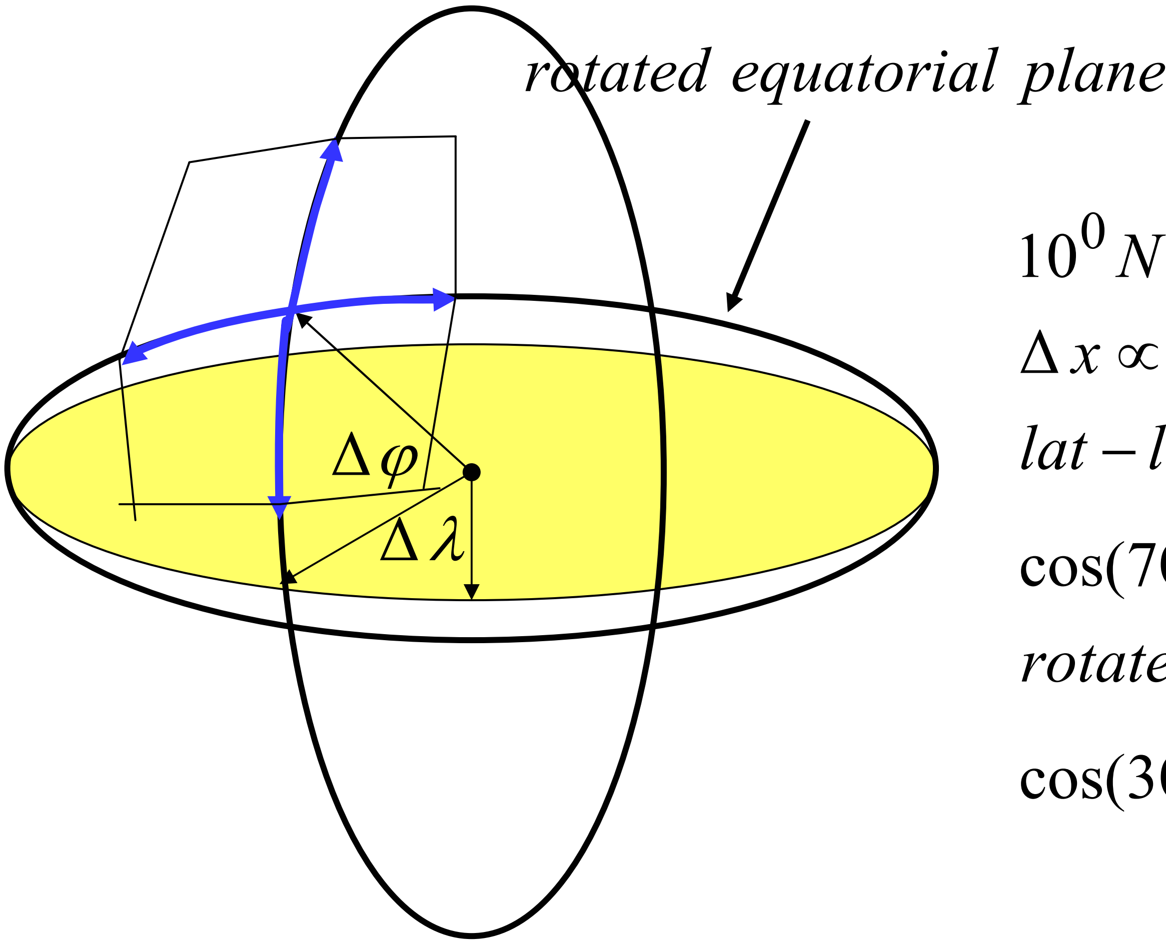

$$10^0 N < \varphi < 70^0 N$$

$$\Delta x \propto \cos(\varphi)$$

$$lat - lon$$

$$\cos(70^0)/\cos(10^0) = 0.3473$$

$$rotated\ lat - lon$$

$$\cos(30^0)/\cos(0^0) = 0.866$$

More uniform grid, longer time steps!

```
      subroutine tll(almd,aphd,tlm0d,ctph0,stph0,tlm,tph)
!     *****************************************************************
!     *                                                               *
!     *  programer: z. janjic, shmz, feb. 1981                        *
!     *  ammended:  z. janjic, ncep, jan. 1996                        *
!     *                                                               *
!     *  transformation from lat-lon to rotated lat-lon coordinates  *
!     *****************************************************************
!     *****************************************************************
!     *  tlm   - transformed longitude, rad.                          *
!     *  tph   - transformed latitude, rad.                           *
!     *  tlm0d - the angle of rotation of the transformed lat-lon    *
!     *          system in the longitudinal direction, degs           *
!     *  ctph0 - cos(tph0), tph0 is the angle of rotation of the     *
!     *          transformed lat-lon systemn in the latitudinal      *
!     *          direction, precomputed                               *
!     *  stph0 - sin(tph0), tph0 is the angle of rotation of the     *
!     *          transformed lat-lon systemn in the latitudinal      *
!     *          direction, precomputed                               *
!     *  almd  - geographical longitude, degs, range -180.,180       *
!     *  aphd  - geographical latitude,  degs, range - 90., 90.,     *
!     *          poles are singular                                   *
!     *****************************************************************
!
      parameter(dtr=3.1415926535897932384626433832795/180.)
!
      relm=(almd-tlm0d)*dtr
      srlm=sin(relm)
      crlm=cos(relm)
      aph=aphd*dtr
      sph=sin(aph)
      cph=cos(aph)
      cc=cph*crlm
      anum=cph*srlm
      denom=ctph0*cc+stph0*sph
!
      tlm=atan2(anum,denom)
      arg=ctph0*sph-stph0*cc
      if(arg.lt.-1.) arg=-1.
      if(arg.gt. 1.) arg= 1.
      tph=asin(arg)
!
      return
      end
```

$$\lambda' = \arctan\left[\frac{\cos(\varphi)\sin(\lambda-\lambda_0)}{\cos(\varphi_0)\cos(\varphi)\cos(\lambda-\lambda_0)+\sin(\varphi_0)\sin(\varphi)}\right]$$

$$\varphi' = \arcsin\left[\cos(\varphi_0)\sin(\varphi)-\sin(\varphi_0)\cos(\varphi)\cos(\lambda-\lambda_0)\right]$$

```
      subroutine rtll(tlm,tph,tlm0d,ctph0,stph0,almd,aphd)
!     *****************************************************************
!     *                                                               *
!     *  programer: z. janjic, shmz, feb. 1981                        *
!     *  ammended:  z. janjic, ncep, jan. 1996                        *
!     *                                                               *
!     *  transformation from rotated lat-lon to lat-lon coordinates   *
!     *****************************************************************
!     *****************************************************************
!     *  tlm   - transformed longitude, rad.                          *
!     *  tph   - transformed latitude, rad.                           *
!     *  tlm0d - the angle of rotation of the transformed lat-lon     *
!     *          system in the longitudinal direction, degs           *
!     *  ctph0 - cos(tph0), tph0 is the angle of rotation of the      *
!     *          transformed lat-lon systemn in the latitudinal       *
!     *          direction, precomputed                               *
!     *  stph0 - sin(tph0), tph0 is the angle of rotation of the      *
!     *          transformed lat-lon systemn in the latitudinal       *
!     *          direction, precomputed                               *
!     *  almd  - geographical longitude, degs, range -180.,180        *
!     *  aphd  - geographical latitude,  degs, range - 90., 90.,      *
!     *          poles are singular                                   *
!     *****************************************************************
!
      parameter(dtr=3.1415926535897932384626433832795/180.)
!
      stlm=sin(tlm)
      ctlm=cos(tlm)
      stph=sin(tph)
      ctph=cos(tph)
!
      sph=ctph0*stph+stph0*ctph*ctlm
      sph=min(sph,1.)
      sph=max(sph,-1.)
      aph=asin(sph)
      aphd=aph/dtr
      anum=ctph*stlm
      denom=(ctlm*ctph-stph0*sph)/ctph0
      relm=atan2(anum,denom)
      almd=relm/dtr+tlm0d
!
      if(almd.gt. 180.)    almd=almd-360.
      if(almd.lt.-180.)    almd=almd+360.
!
      return
      end
```

$$\varphi = \arcsin\left[\cos(\varphi_0)\sin(\varphi') + \sin(\varphi_0)\cos(\varphi')\cos(\lambda')\right]$$

$$\lambda = \arctan\left[\frac{\cos(\varphi')\sin(\lambda')}{\dfrac{\cos(\varphi')\cos(\lambda') - \sin(\varphi_0)\sin(\varphi)}{\cos(\varphi_0)}}\right] + \lambda_0$$

Velocity components must be rotated as well!

➢ Pressure-sigma hybrid (Arakawa and Lamb, 1977).

- Nondivergent flow on pressure surfaces
- Flat coordinate surfaces at high altitudes where sigma problems worst (Simmons and Burridge, 1981)
- Higher vertical resolution over elevated terrain
- No discontinuities and internal boundary conditions

➢ Hybrid vertical coordinate

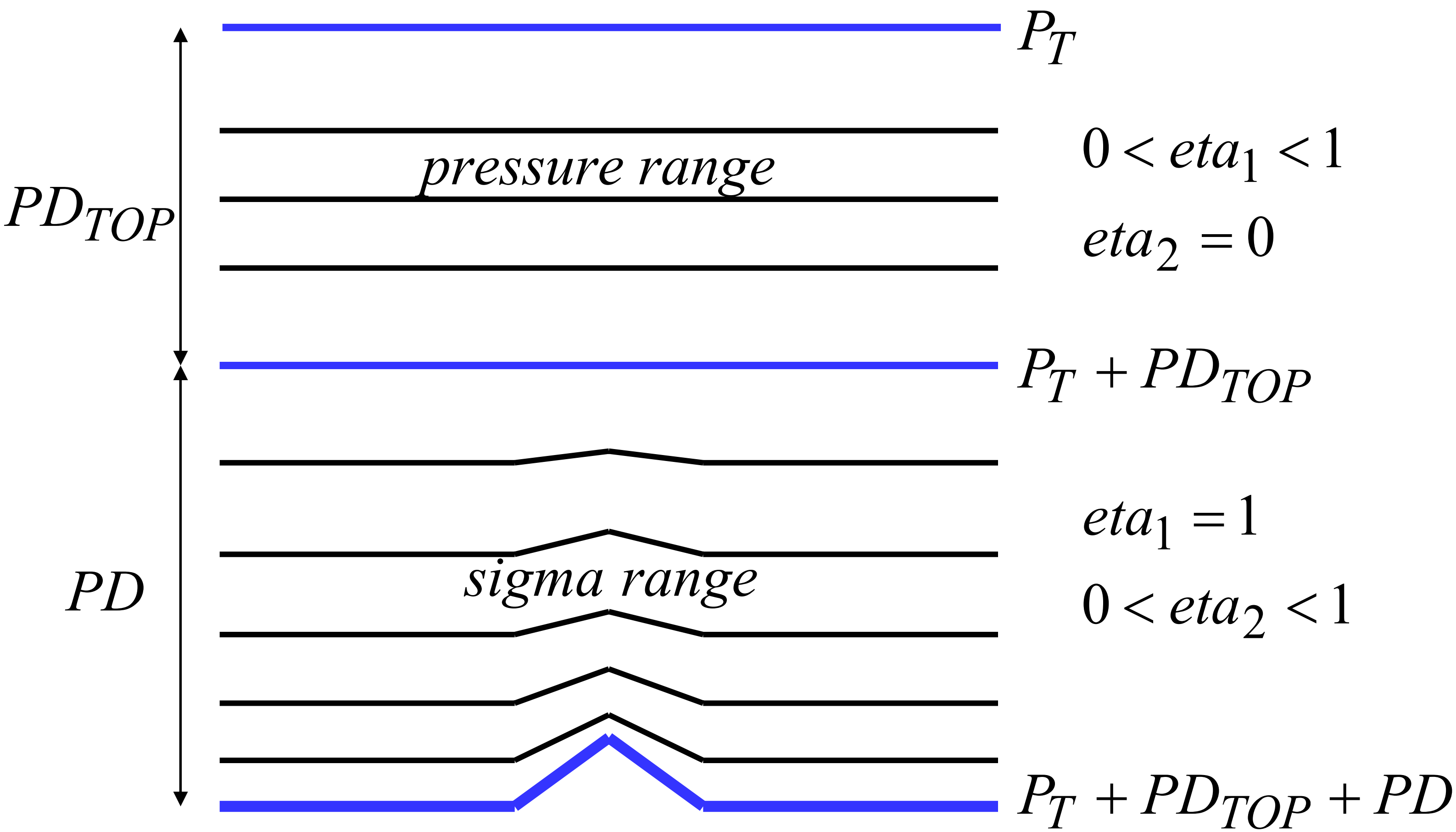

$$p = eta_1\, PD_{TOP} + eta_2\, PD + P_T$$

➢ Equations in hybrid coordinate

$$\frac{\partial PD}{\partial t} + \nabla_\sigma \bullet (PD\ \mathbf{v}) + \frac{\partial (PD\ \dot{\sigma})}{\partial \sigma} = 0$$

$$\nabla_p \bullet (\mathbf{v}) + \frac{\partial \omega}{\partial p} = 0$$

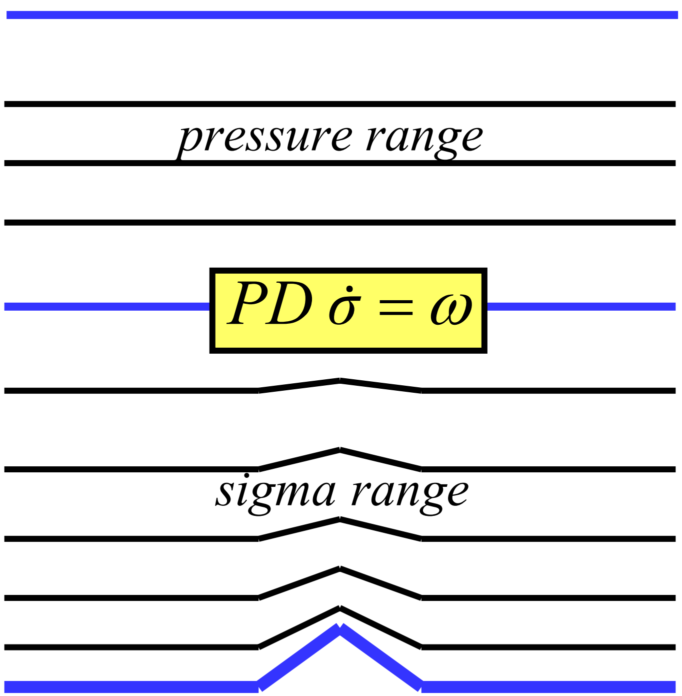

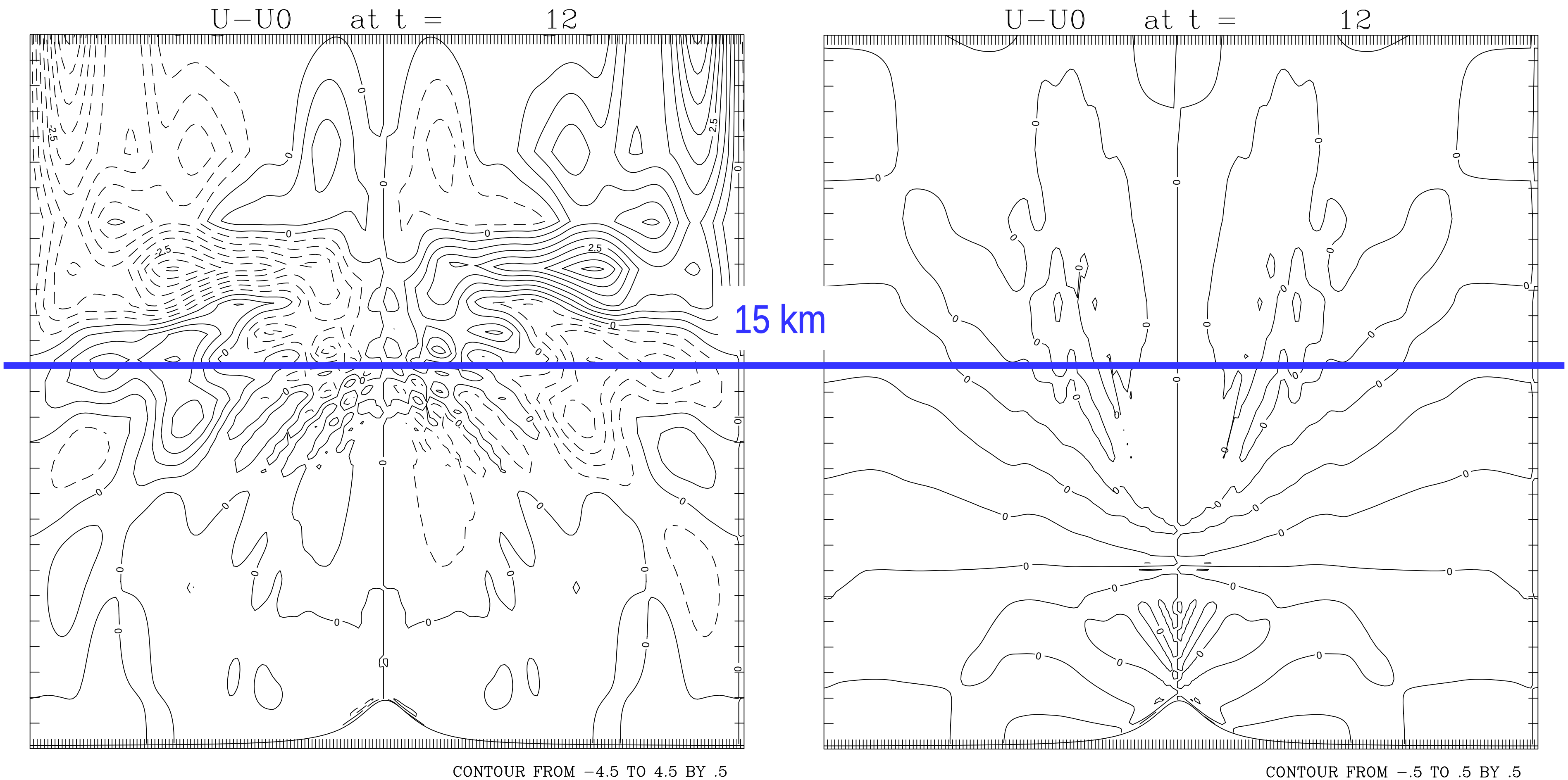

Wind component developing due to the spurious pressure gradient force in the sigma coordinate (left panel), and in the hybrid coordinate with the boundary between the pressure and sigma domains at about 400 hPa (right panel). Dashed lines represent negative values.

Example of nonphysical small scale energy source

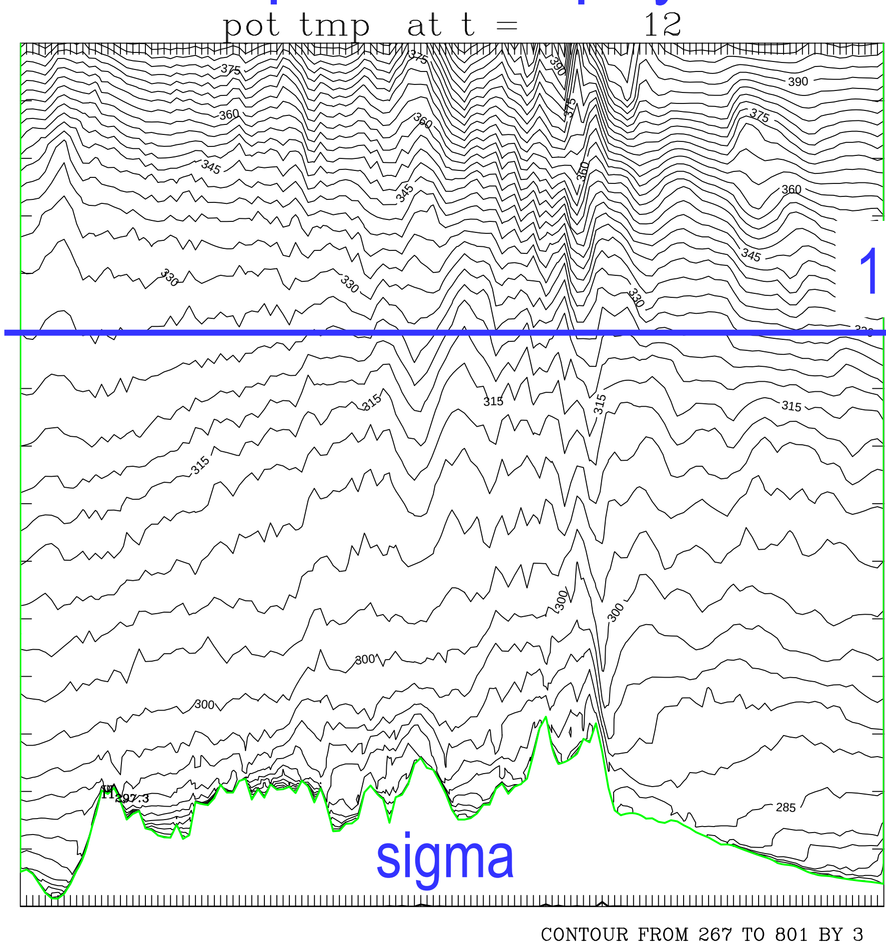

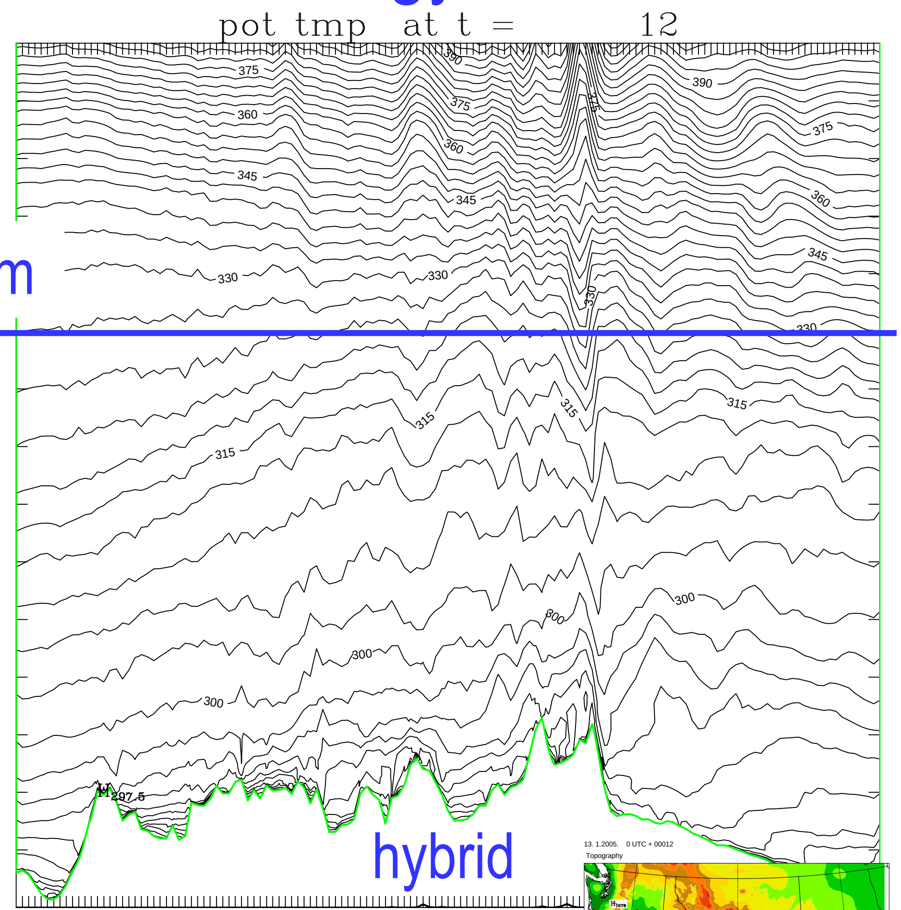

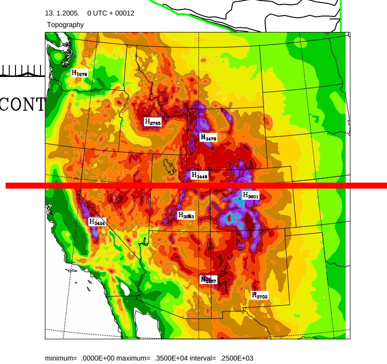

Potential temperature, January 13, 2005, 00Z
12 hour forecasts, 3 deg contours

- Basic discretization principle is conservation of important properties of the continuous system.

  - “Mimetic” approach

    http://www.math.unm.edu/~stanly/mimetic.html

  - Major novelty in applied mathematics, …

  - … but well established in atmospheric modeling (Arakawa, 1966, 1972, 1977 …; Sadourny, 1975 …; Janjic, 1977, 1984 …; …)

➢ Criteria chosen

- Energy and enstrophy conservation in order to control nonlinear energy cascade
- A number of first order and quadratic quantities conserved
- A number of properties of differential operators preserved
- Omega-alpha term, consistent transformations between KE and PE
- Minimized errors due to representation of orography

- Arakawa criteria for choosing grid, large scales:
  - Geostrophic adjustment
  - Nonlinear quasi-nondivergent flow
- Gravity-inertia wave frequencies on rectangular grids with 2nd order finite differencing (Winninghoff 1968; Arakawa and Lamb 1977, MCP; Janjic 1984, MWR; Randall, 1994, MWR; Gavrilov, 2004, MWR), classical synoptic scale design

h		h		h
	$\mathbf{v}$		$\mathbf{v}$	
h		h		h
	$\mathbf{v}$		$\mathbf{v}$	
h		h		h

B

h	u	h	u	h
v		v		v
h	u	h	u	h
v		v		v
h	u	h	u	h

C

h	$\mathbf{v}$	h	$\mathbf{v}$
$\mathbf{v}$	h	$\mathbf{v}$	h
h	$\mathbf{v}$	h	$\mathbf{v}$
$\mathbf{v}$	h	$\mathbf{v}$	h

E

h,χ,ψ	h,χ,ψ	h,χ,ψ
h,χ,ψ	h,χ,ψ	h,χ,ψ
h,χ,ψ	h,χ,ψ	h,χ,ψ

B'/Z

Janjic 1984; Randall 1994;
Gavrilov 2004, MWR

➢ Problems due to averaging

- C grid problems in the entire admissible wavenumber range with group velocity of gravity-inertia waves in case of coarse resolution or weak static stability due to averaging of Coriolis force

- B/E grid problems with small-scale low-frequency noise due to averaging of divergence component terms

Mesoscales, linearized anelastic nonhydrostatic Eqs:

$$X = kd \quad Y = ld \quad Z = m\Delta z$$

$$\left(\frac{\upsilon}{f}\right)^2 = \frac{\left(\frac{N}{f}\right)^2 (X^2 + Y^2) + Z^2 \left(\frac{d}{\Delta z}\right)^2}{X^2 + Y^2 + Z^2 \left(\frac{d}{\Delta z}\right)^2}$$

$$\left(\frac{\upsilon_B}{f}\right)^2 = \frac{\left(\frac{N}{f}\right)^2 \cos^2\left(\frac{Z}{2}\right)\left[\boxed{\cos^2\left(\frac{Y}{2}\right)}\sin^2\left(\frac{X}{2}\right) + \boxed{\cos^2\left(\frac{X}{2}\right)}\sin^2\left(\frac{Y}{2}\right)\right] + \boxed{\left(\frac{d}{\Delta z}\right)^2}\sin^2\left(\frac{Z}{2}\right)}{\boxed{\cos^2\left(\frac{Y}{2}\right)}\sin^2\left(\frac{X}{2}\right) + \boxed{\cos^2\left(\frac{X}{2}\right)}\sin^2\left(\frac{Y}{2}\right) + \left(\frac{d}{\Delta z}\right)^2 \sin^2\left(\frac{Z}{2}\right)^2}$$

$$\left(\frac{\upsilon_C}{f}\right)^2 = \frac{\left(\frac{N}{f}\right)^2 \cos^2\left(\frac{Z}{2}\right)\left[\sin^2\left(\frac{X}{2}\right) + \sin^2\left(\frac{Y}{2}\right)\right] + \boxed{\left(\frac{d}{\Delta z}\right)^2}\boxed{\cos^2\left(\frac{X}{2}\right)\cos^2\left(\frac{Y}{2}\right)}\sin^2\left(\frac{Z}{2}\right)}{\sin^2\left(\frac{X}{2}\right) + \sin^2\left(\frac{Y}{2}\right) + \left(\frac{d}{\Delta z}\right)^2 \sin^2\left(\frac{Z}{2}\right)^2}$$

(Communicated by Klemp)

Predominantly stable stratification on large scales

Weak stability - important motions on meso scales

$$f = 0.0001,\ N = 0.0001,\ d/\Delta z = 30,\ Z = \pi/32$$

$$\frac{\nu}{f} = \frac{\nu_B}{f} = 1; \quad \nu_C :$$

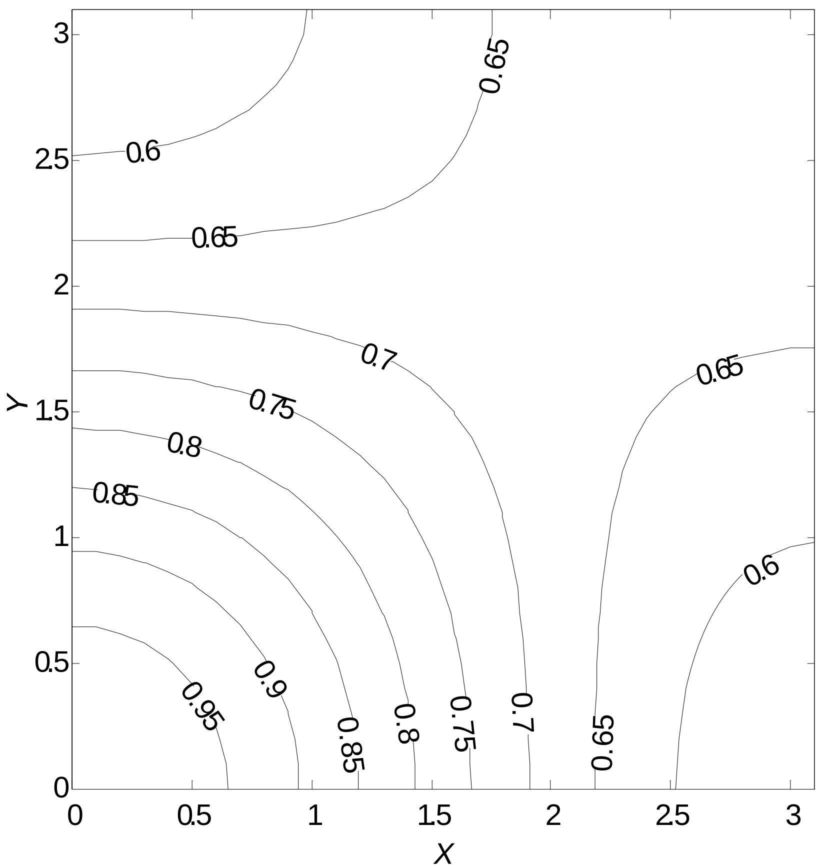

How bad is the B/E grid problem? Synoptic scale, 30 km resolution.

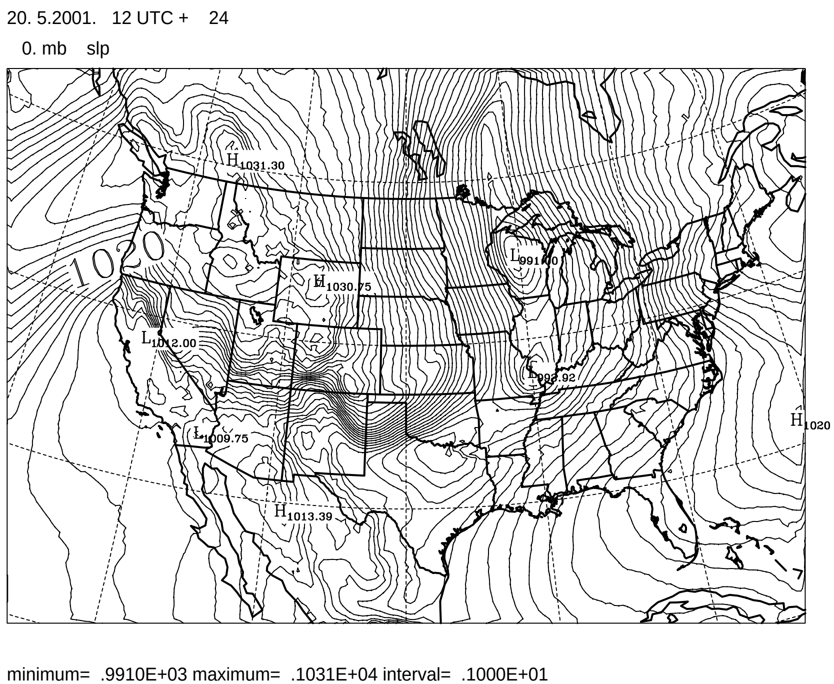

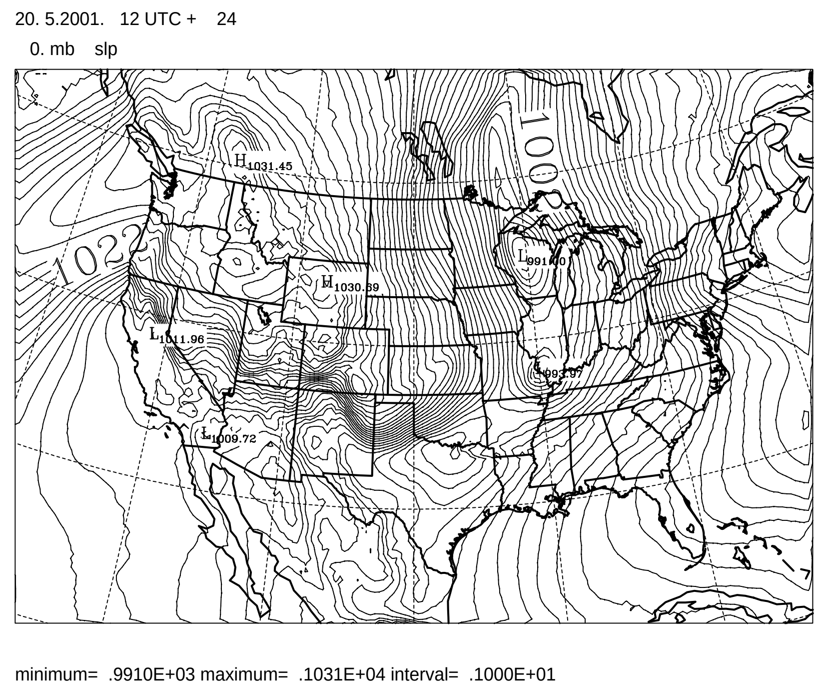

Nothing

Compact, corrected freq.

- C grid: possible problems with all waves
- B grid: problems with short waves (hard to see)
  - Large Rossby numbers
  - Efficient B/E grid filtering technique (Janjic, 1979)
- Advantage B/E grid
- E grid initial formulation (ESMF compliant unified B grid model also under development).

- Nonlinear terms
  - Due to nonlinearity, numerical models generally generate excessive small scale noise
  - A major noise source is false nonlinear energy cascade (Phillips, 1954; Arakawa, 1966 … ; Sadourny, 1975; …)
  - Accumulation of energy at small scales, distortion of spectrum and nonlinear instability
- Other computational errors as noise sources (e.g. sigma coordinate)

- Historically, the problem controlled by:
  - Removing spurious small scale energy by filtering, dissipation
  - Preventing excessive noise generation by enstrophy and energy conservation (Arakawa, 1966 …)

Classical paper by Sadourny, 1975, JAS:

the "inertial" range; however, a correct energy spectrum for a numerical solution is not by itself a proof of the accuracy of the simulated energy transfers. In fact, it is always possible to force the energy distribution of any numerical solution to conform to a known spectral shape in the inertial range through ad-hoc assumptions, regarding, for instance, addition of artificial viscosity. However, if we are to trust numerical modelling as a method for providing better understanding of the real processes, we must then admit that a realistic energy spectrum should not be forced by artificial techniques, but should come instead as a by-product of the first principles only, via correct treatment of the nonlinear interactions. More precisely, accurate long-term statistical distributions of kinetic energy should result from:

1) An accurate distribution of sources and sinks (outside the inertial range).

2) Accurate representation of the statistical transfers of energy within the resolved scales ("internal" transfers) in spite of the truncation error of the finite-difference scheme in the smaller scales.

3) An accurate parameterization of the statistical effects of nonlinear interactions with the subgrid-scale motions.

- It is important that the statistical properties of the spectrum be obtained in a physically correct way!

Nonlinear Advection Schemes and Energy Cascade on Semi-Staggered Grids

ZAVIŠA I. JANJIĆ

Federal Hydrometeorological Institute, Belgrade, Yugoslavia

(Manuscript received 4 October 1982, in final form 29 February 1984)

ABSTRACT

A common problem with nonlinear advection schemes is the false accumulation of energy at the smallest resolvable scales. To keep this process under control, following Arakawa (1966), a number of energy and enstrophy conserving schemes for staggered and semi-staggered grids have been designed. In this paper, it is demonstrated that, in contrast to the staggered grid, the conservation of energy and enstrophy on the semi-staggered grids does not guarantee that the erroneous transport of energy from large to small scales will be effectively restricted.

Using a new approach to the application of the Arakawa Jacobian, a scheme for a semi-staggered grid which exactly reflects the Arakawa theory for nondivergent flow is obtained for the first time. This is achieved by conservation of energy and enstrophy as defined on the staggered grid. These two quantities are of higher accuracy and cannot be calculated directly from the dependent variables on the semi-staggered grid. It is further demonstrated that the amount of energy which can be transported toward smaller scales is more restricted than for any other scheme of this type on both staggered and semi-staggered grids.

Experiments performed with the proposed scheme and a scheme which conserves energy and enstrophy as defined on the semi-staggered grid reveal visible differences in long-term integrations which are in agreement with the theory and demonstrate the advantages of the new scheme.

Very interesting possibilities on the E grid!

- Barotropic nondivergent vorticity Eq., Charney, Fjortoft & von Neumann started NWP from

$$\frac{\partial \zeta}{\partial t} + J(\psi, \zeta) = 0, \quad \zeta = \nabla^2 \psi$$

- Essence of large scale atmospheric flow regime

$$\overline{\psi \frac{\partial \zeta}{\partial t}} = -\overline{\psi\, J(\psi, \zeta)} = 0$$

$$\overline{\zeta \frac{\partial \zeta}{\partial t}} = -\overline{\zeta\, J(\psi, \zeta)} = 0$$

$$\overline{K} = \overline{\frac{1}{2}(\nabla \psi)^2} = const, \quad \overline{\eta} = \overline{\frac{1}{2}(\nabla^2 \psi)^2} = const$$

ψ_n orthogonal functions, Parseval theorem,

$$\overline{K} = \frac{1}{2}\sum_n \boxed{\lambda_n^2} \psi_n^2 = const, \quad \overline{\eta} = \frac{1}{2}\sum_n \lambda_n^4 \psi_n^2 = const$$

Eigenvalues of Laplacian

$$\overline{K} = \frac{1}{2}\sum_n K_n = const, \quad \overline{\eta} = \frac{1}{2}\sum_n \boxed{\lambda_n^2} K_n = const$$

$$\overline{\lambda^2} = \frac{\overline{\eta}}{\overline{K}} = \frac{\sum_n \lambda_n^2 K_n}{\sum_n K_n} = const$$

$$\boxed{\overline{\lambda^2}}\,\overline{K} = \sum_n \boxed{\lambda_n^2} K_n$$

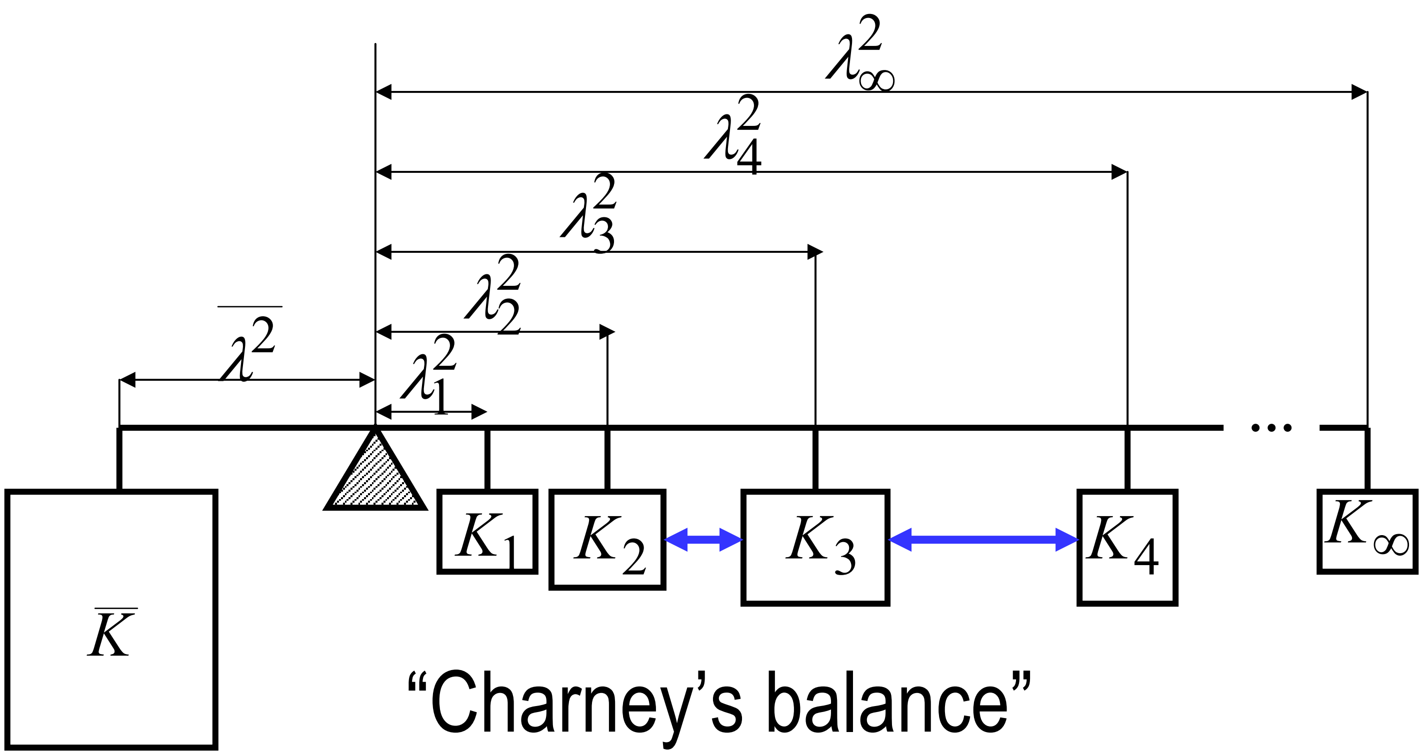

"Charney's balance"

$$\Delta K_1 + \Delta K_2 + \Delta K_3 = 0$$

$$\lambda_1^2 \Delta K_1 + \lambda_2^2 \Delta K_2 + \lambda_3^2 \Delta K_3 = 0$$

$$\lambda_1^2 < \lambda_2^2 < \lambda_3^2$$

$$\Delta K_1 = -\frac{(\lambda_3^2 - \lambda_2^2)}{(\lambda_3^2 - \lambda_1^2)} \Delta K_2$$

$$\Delta K_3 = -\frac{(\lambda_2^2 - \lambda_1^2)}{(\lambda_3^2 - \lambda_1^2)} \Delta K_2$$

- Triads, Fjortoft's theorem
- Downscale energy cascade restricted!
- Fundamental property of the fluid!

➢ Definitions of energy, vorticity, eigenvalues of Laplacian?

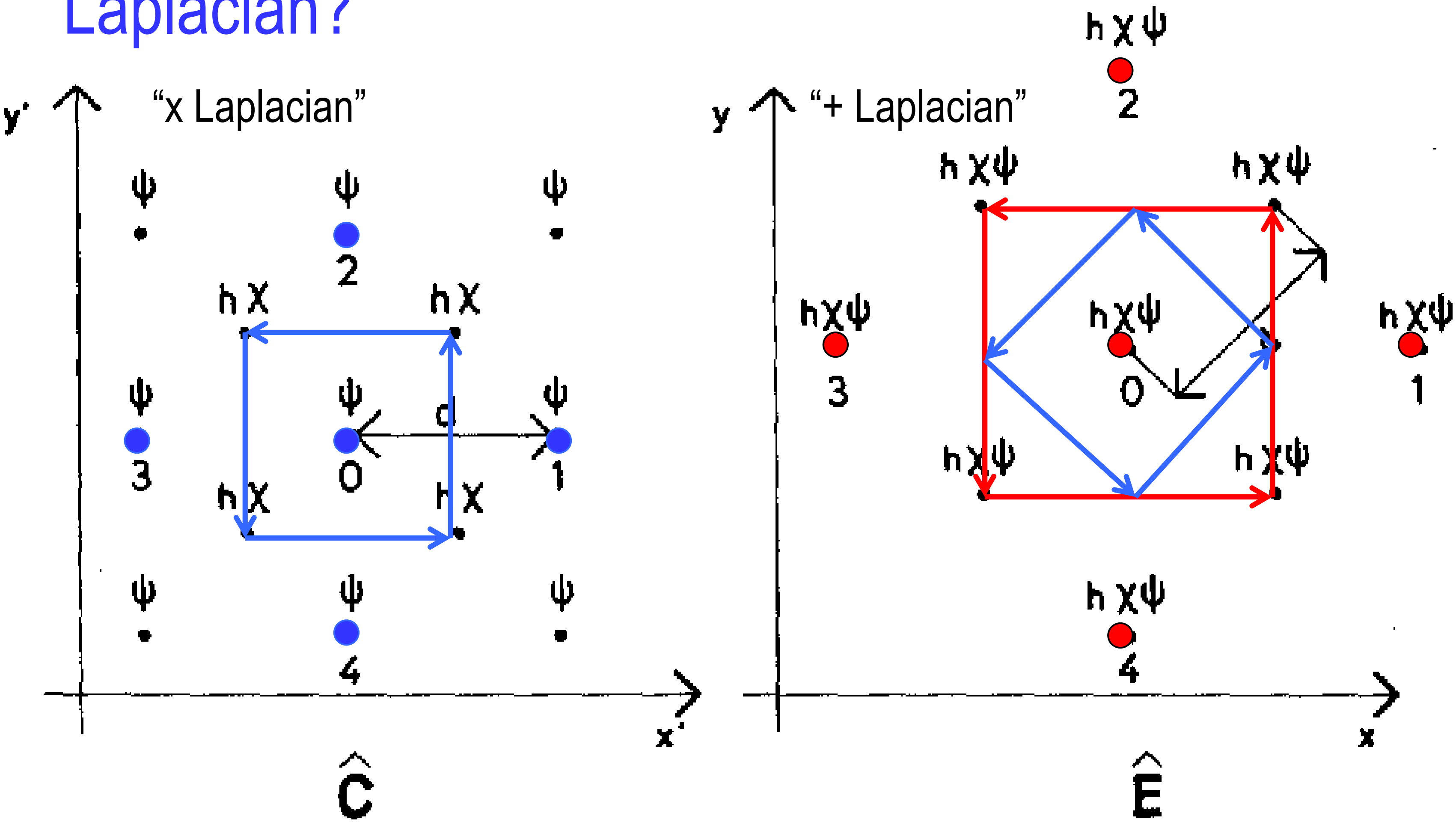

FIG. 2. Distributions of variables over grid points Ĉ and Ê with associated coordinate systems.

Eigenvalues of "x Laplacian"

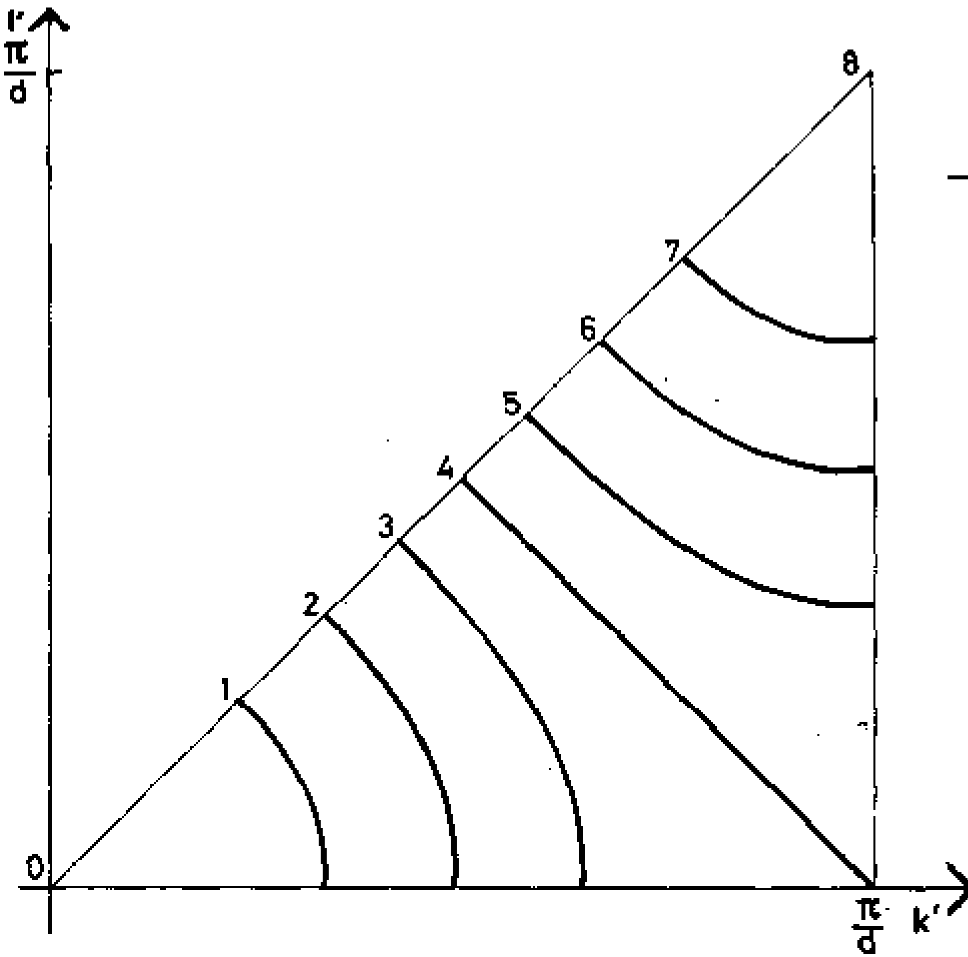

FIG. 3. Eigenvalues of the finite difference Laplacian ∇_x^2. The values are nondimensionalized by multiplication by d^2.

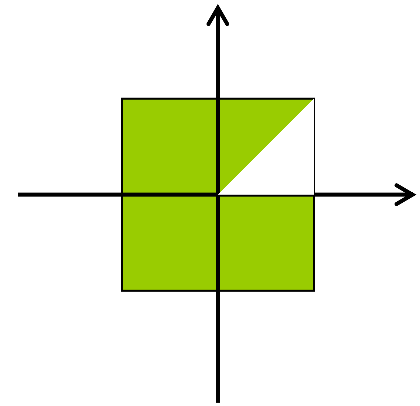

Eigenvalues of
"+ Laplacian"

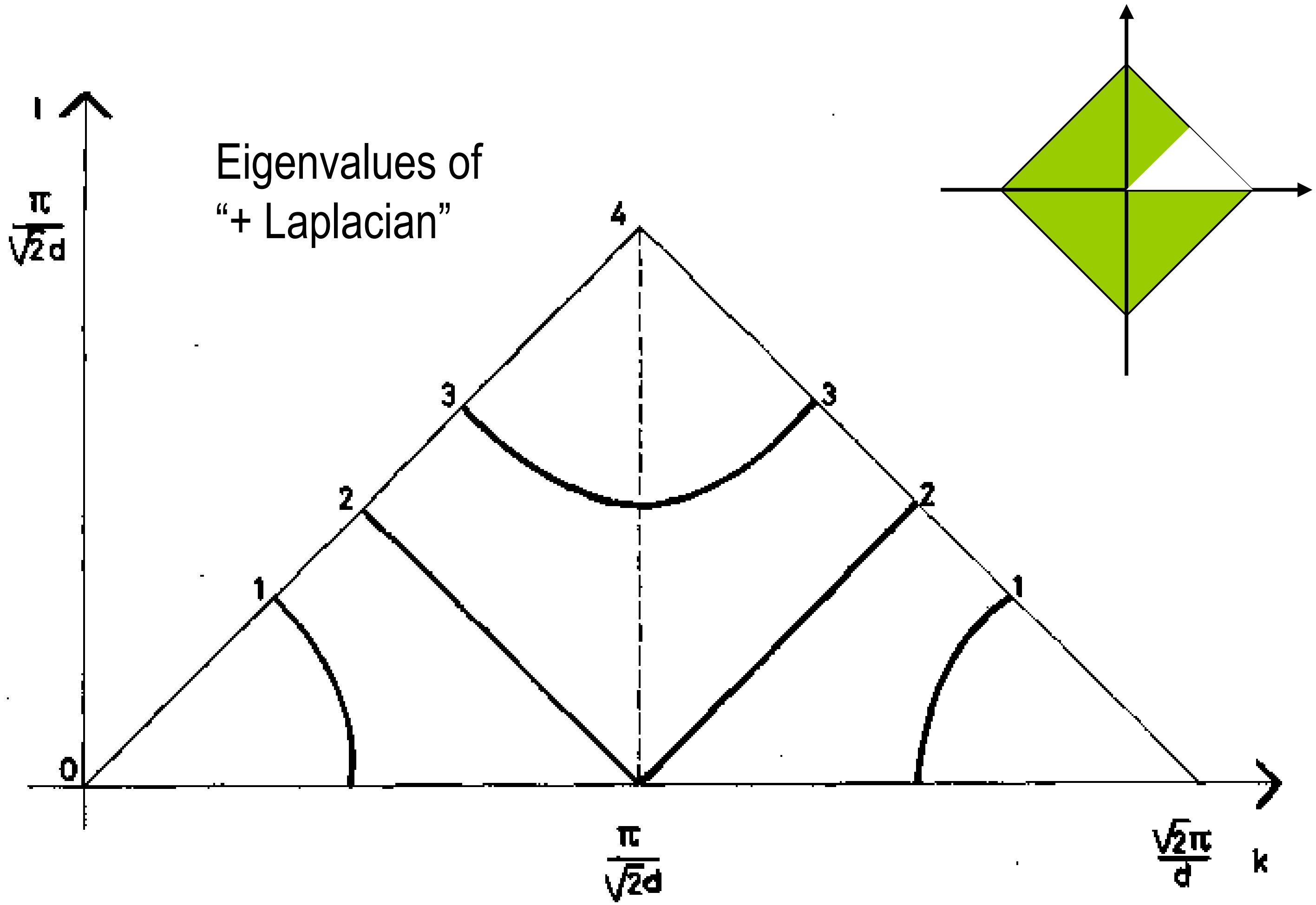

FIG. 5. Eigenvalues of the finite difference Laplacian ∇_+^2. The values are nondimensionalized by multiplication by d^2.

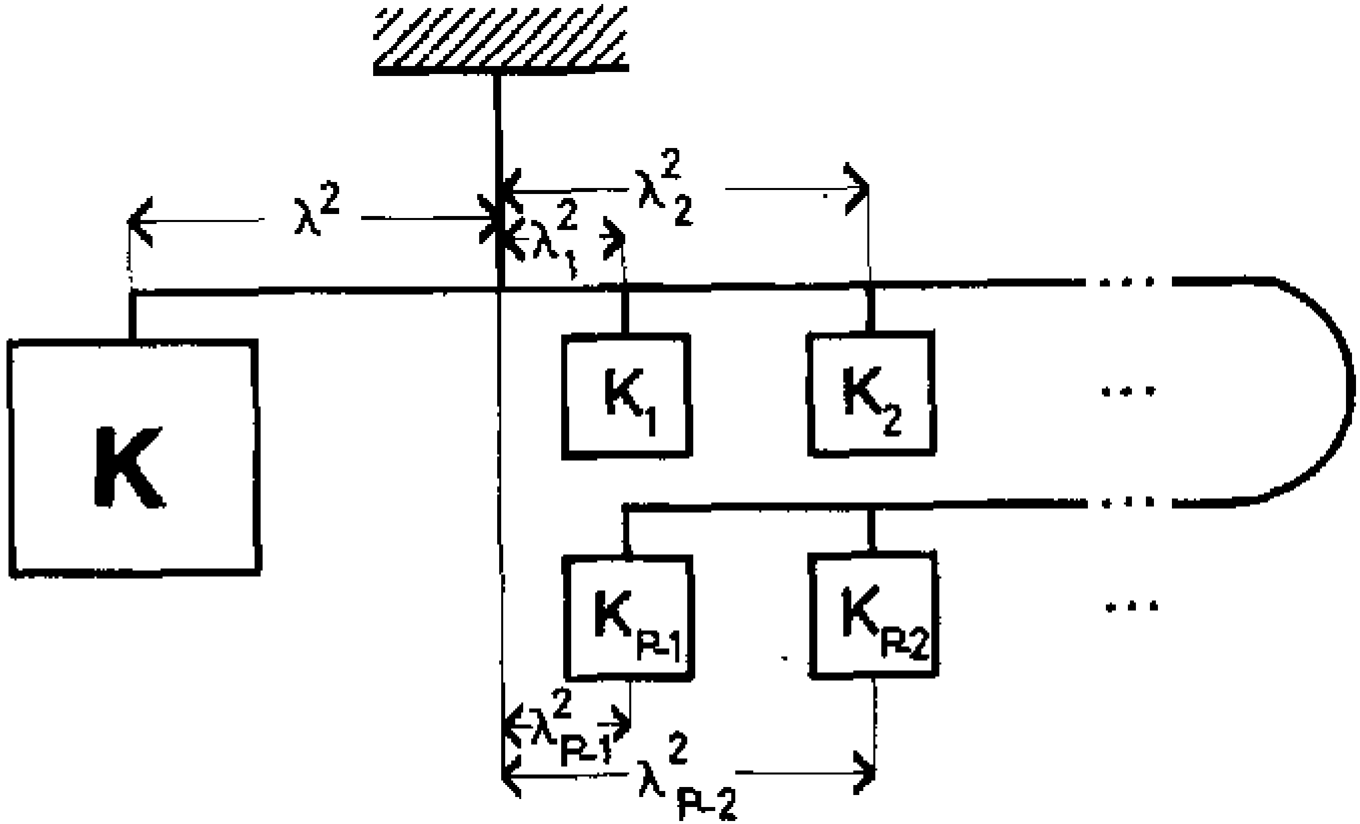

FIG. 6. Schematic representation of the limitations imposed on the nonlinear energy cascade by the energy and enstrophy conservation on the E grid.

$$\frac{\partial}{\partial t}(-\delta_y\psi) = -\frac{\sqrt{2}}{2}[\overline{J_A(\bar{\psi}^{y'}, -\delta_{y'}\psi)}^{x'}$$

$$-\overline{J_A(\bar{\psi}^{x'}, \delta_{x'}\psi)}^{y'}] + \frac{\sqrt{2}}{2}(\overline{R'}^{x'} - \overline{S'}^{y'}), \quad (34)$$

$$\frac{\partial}{\partial t}(\delta_x\psi) = -\frac{\sqrt{2}}{2}[\overline{J_A(\bar{\psi}^{y'}, -\delta_{y'}\psi)}^{x'}$$

$$+\overline{J_A(\bar{\psi}^{x'}, \delta_{x'}\psi)}^{y'}] + \frac{\sqrt{2}}{2}(\overline{R'}^{x'} + \overline{S'}^{y'}). \quad (35)$$

On the left-hand sides of (34) and (35) we recognize the time derivatives of the E-grid nondivergent velocity components.

$$\frac{\partial}{\partial t}(-\delta_y \psi) = -J_A(\bar{\psi}^x, -\delta_y \psi) + \frac{\sqrt{2}}{2}(R'^{x'} - S'^{y'}). \quad (48)$$

$$\frac{\partial}{\partial t}(\delta_x \psi) = -J_A(\bar{\psi}^y, \delta_x \psi) + \frac{\sqrt{2}}{2}(R'^{x'} + S'^{y'}). \quad (49)$$

- Can be done exactly for the E grid velocity components on the E grid in spherical geometry (Janjic, 1984, MWR)!

- Can be done exactly for a linear combination of velocity components and map factors on the B grid in spherical geometry

Distances of weights on Charney balance with Janjic (1984) scheme

Definite advantage of E(B) grid over the C grid!

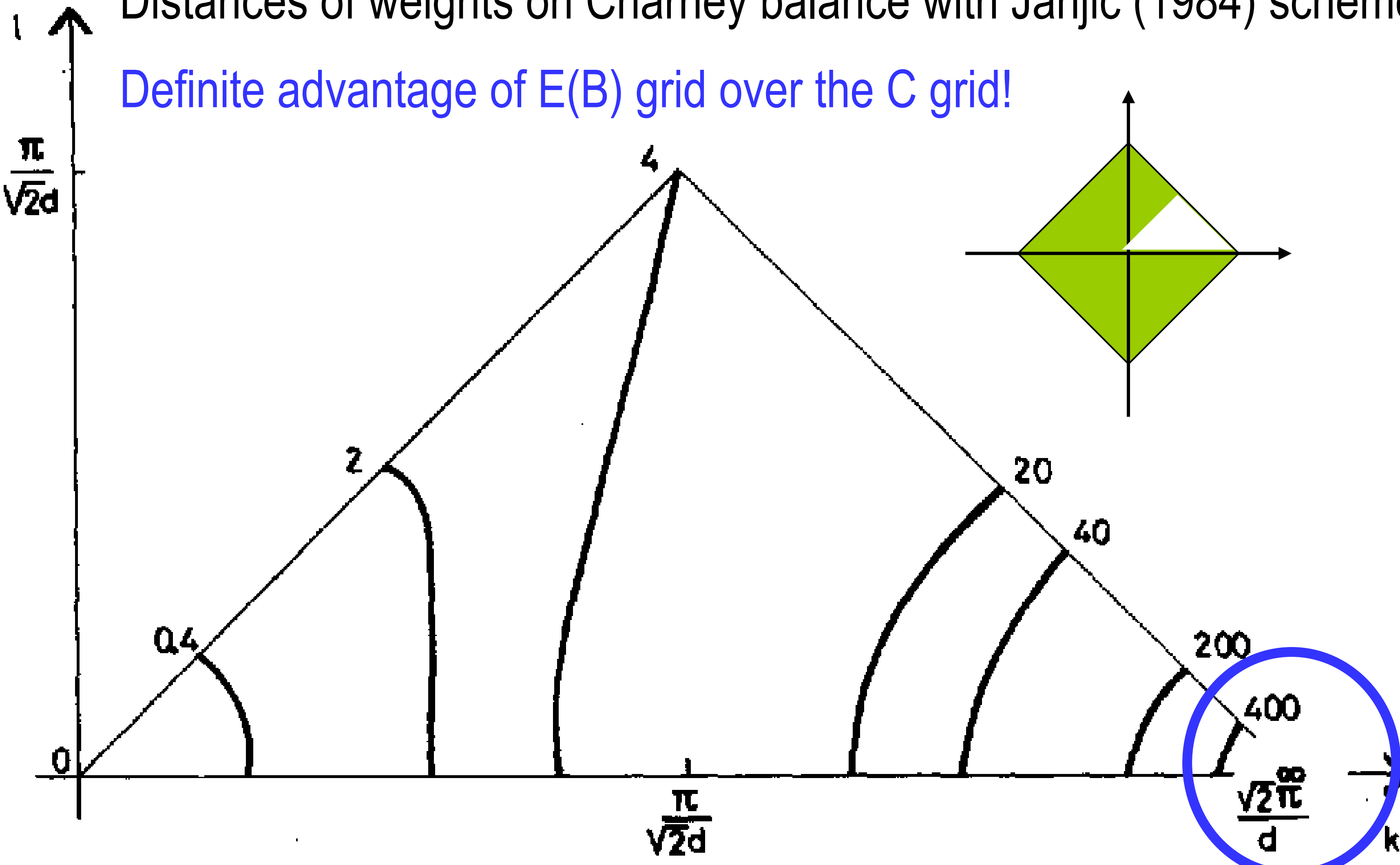

FIG. 9. The analogs of the eigenvalues of a finite difference Laplacian for a scheme which conserves E-grid energy and C-grid enstrophy. The values are nondimensionalized by multiplication by d^2.

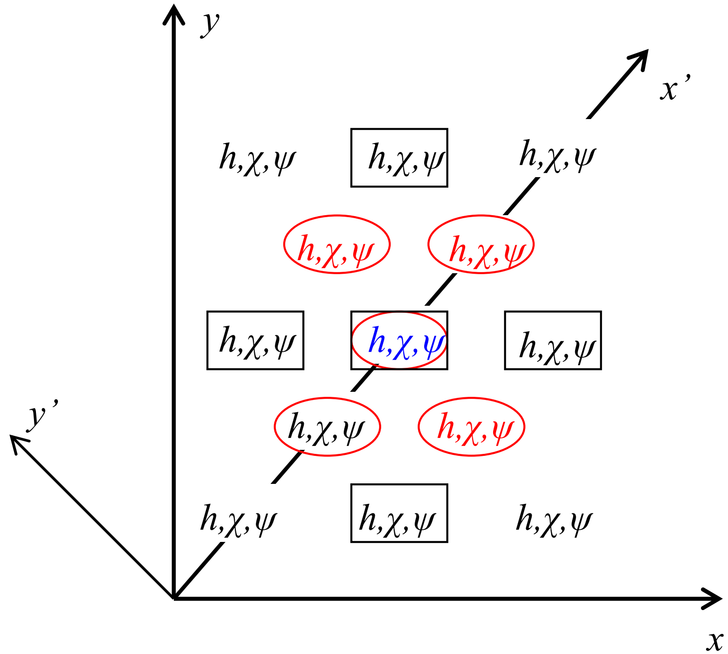

- Rotational flow and cyclic boundary conditions
  - Enstrophy as defined on grid C conserved on E grid

$$\sum_{i,j}(\delta_{x'x'}\psi+\delta_{y'y'}\psi)^2\Delta A$$

  - Rotational energy as defined on grid C conserved on E grid

$$\sum_{i,j}\frac{1}{2}(\delta_{y'}\psi)^2\Delta A+\sum_{i,j}\frac{1}{2}(\delta_{x'}\psi)^2\Delta A$$

- Rotational momentum as defined on grid C conserved on grid E

- Rotational energy as defined on grid E conserved

$$\sum_{i,j} \frac{1}{2}[\delta_y \psi^2 + \delta_x \psi^2]\Delta A$$

- Rotational momentum as defined on grid E conserved

➢ General flow:

- Kinetic energy as defined on grid E conserved

$$\sum \frac{1}{2}[(\delta_x \phi - \delta_y \psi)^2 + (\delta_y \phi + \delta_x \psi)^2]\Delta V$$

- Momentum as defined on grid E conserved

- Mass conserved

- In hydrostatic limit, advection of T conserves first and second moments

- Interchangable flux/advective form in horizontal FD, mimetic differencing

- “Isotropicized” horizontal divergence & advection operators on 9-point Arakawa Jacobian stencil

➢ Advection, divergence operators, each point talks to all neighbors

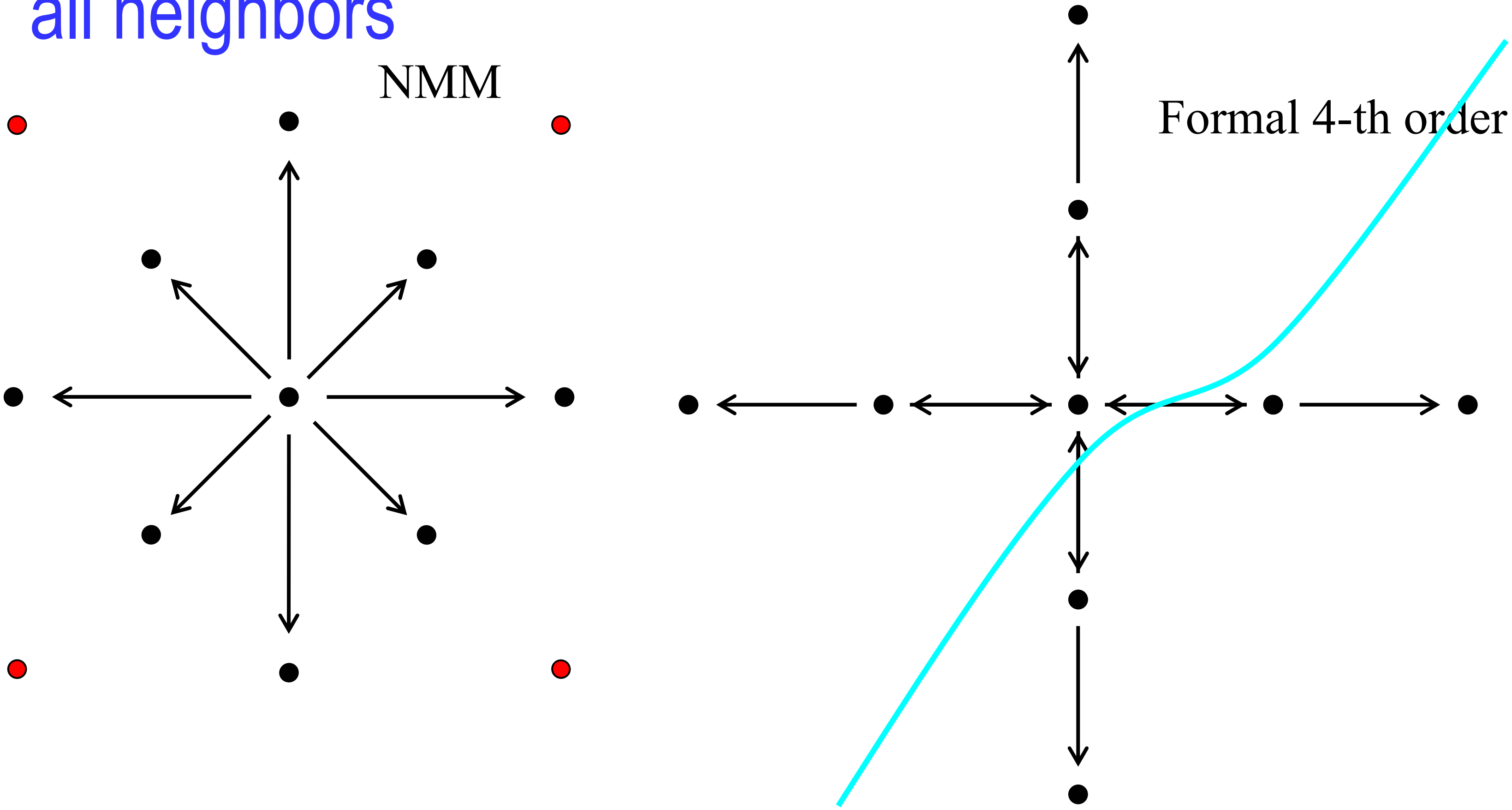

* E grid FD schemes also reformulated for, and used in ESMF compliant B grid model being developed

➢ Higher order formal accuracy?

- 4th order Janjic 1984 scheme already exists, Rancic (1988, MWR)
- Another sophisticated 4th order scheme recently tested
- Higher order of formal accuracy generally used only for advection terms, second order for gravity-inertia terms, overall accuracy still second order
- Higher order of formal accuracy not synonimous with higher accuracy; may be less accurate with noisy data!
- Extra computational boundary conditions required, generally more halo data to exchange (scaling) and more noise

- Problem, advection not clearly separable from "linear" terms beyond shallow water eqs

Second order

$$\frac{d\mathbf{v}}{dt} = -(1+\varepsilon)\nabla_\sigma \Phi - \boxed{\alpha \nabla_\sigma p} + f\mathbf{k}\times\mathbf{v}$$

$$\frac{\partial T}{\partial t} = -\mathbf{v}\bullet\nabla_\sigma T - \dot{\sigma}\frac{\partial T}{\partial \sigma} + \frac{\alpha}{c_p}[\frac{\partial p}{\partial t} + \boxed{\mathbf{v}\bullet\nabla_\sigma p} + \dot{\sigma}\frac{\partial p}{\partial \sigma}]$$

  - For consistency same order of accuracy in the omega-alpha term

- No visible benefit in practice

➢ Lateral boundaries

- Upstream advection in three rows next to the boundary
  - No computational outflow boundary condition for advection
  - Enhanced damping along boundaries

➢Vertical discretization

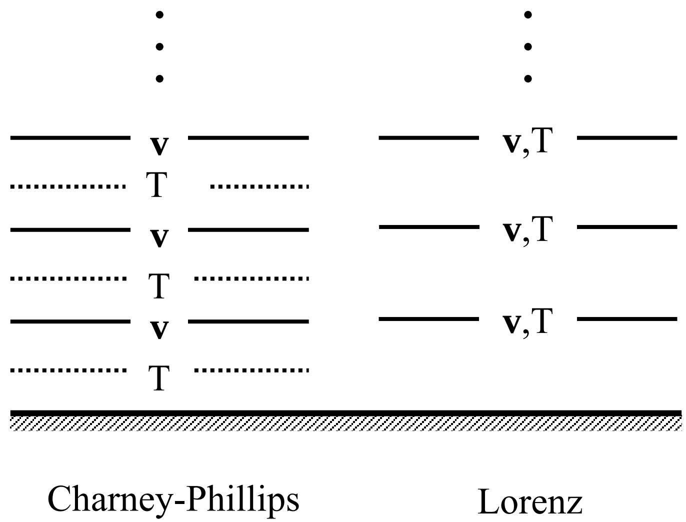

- Quadratic conservative vertical advection of u, v, T

- Time stepping

- Explicit, except for vertically propagating sound waves.

- Different schemes for different processes:
  - Adams-Bashforth for horizontal advection of u, v, T and Coriolis force

$$\frac{y^{\tau+1} - y^{\tau}}{\Delta t} = \frac{3}{2} f(y^{\tau}) - \frac{1}{2} f(y^{\tau-1})$$

    - Slight linear instability, can be tolerated in practice or stabilized by slight off-centering

- Crank-Nicholson for vertical advection of u, v, T

$$\frac{y^{\tau+1}-y^{\tau}}{\Delta t}=\frac{1}{2}[f(y^{\tau+1})+f(y^{\tau})]$$

- Forward-Backward (Ames, 1968; Janjic and Wiin-Nielsen, 1977; Janjic 1979, Beitrage) for fast waves

$$\frac{\partial u}{\partial t}=-g\frac{\partial h}{\partial x},\ \frac{\partial h}{\partial t}=-H\frac{\partial u}{\partial x}$$

$$h^{\tau+1}=h^{\tau}-\Delta t\,H\delta_x u^{\tau},\ u^{\tau+1}=u^{\tau}-\Delta t\,g\delta_x h^{\tau+1}$$

- Implicit for vertically propagating sound waves (Janjic et al., 2001; Janjic, 2003)

➢ No redundant computations, high comp. efficiency.

Janjic et al., 2001, MWR

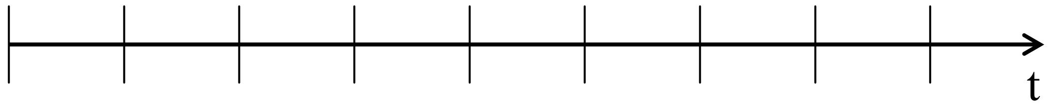

Klemp and Wilhelmson, 1978a, JAS

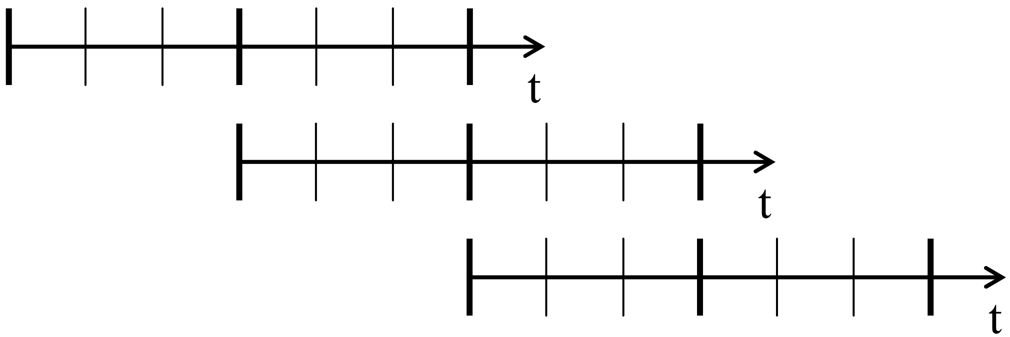

Each interval covered twice,
shorter small time steps on C grid.

Wicker and Skamarock, RK3, 2002, MWR

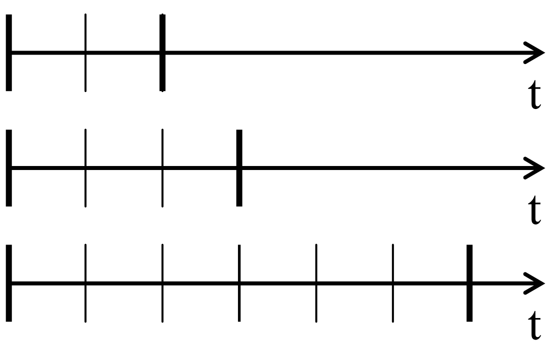

Step 1

Step 2

Step 3

Each interval covered 1.8 times,
shorter small time steps on C grid.

➢ One step loop

- PDTE update hydrostatic pressure, vertical velocity
- ADVE vertical and horizontal advection, Coriolis force
- VTOA vertical part of omega-alpha, incremental update of pressure & temperature
- Nonhydrostatic on/off block
  - VADZ tendency & vertical advection of height
  - HADZ horizontal advection of height
  - EPS dw/dt, ε, vertically propagating sound waves

- Passive substance advection
  - VAD2 vertical
  - HAD2 horizontal
- Physics block
- HDIFF lateral diffusion
- BOCOH update boundary conditions for mass variables

- PFDHT pressure gradient force, incremental update of u & v, divergence, horizontal part of omega-alpha
- DDAMP divergence damping
- BOCOV update boundary conditions for momentum

➢ Formulation reproduces classical 2D nonhydrostatic solutions

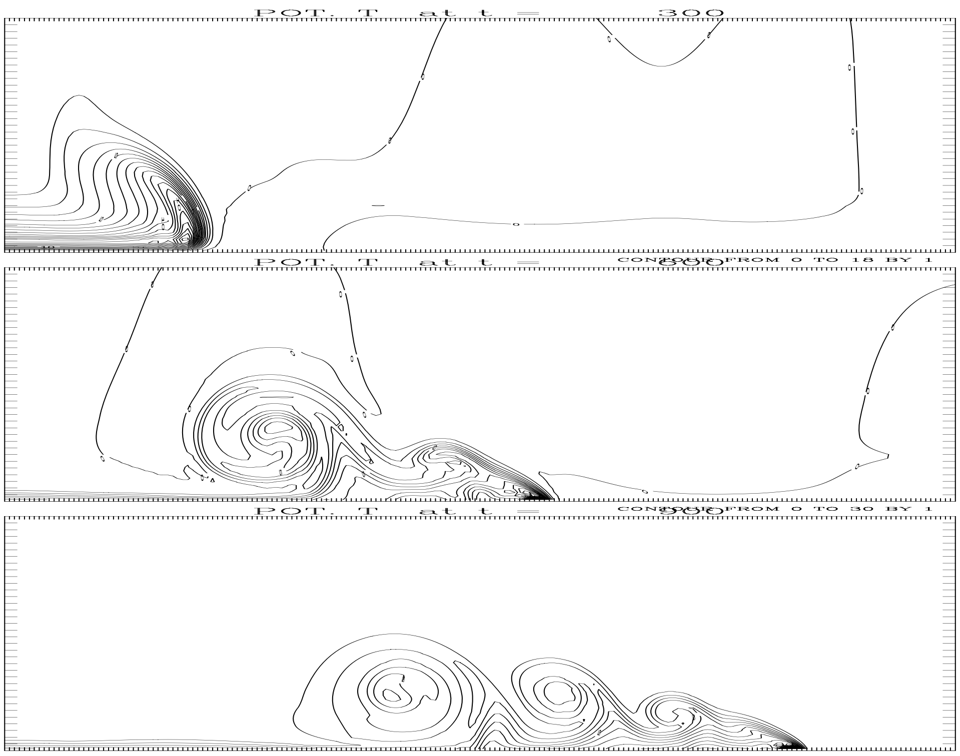

The cold bubble test. Potential temperatures after 300 *s*, 600 *s* and 900 *s* in the right hand part of the integration domain extending from the center to 19200 m, and from the surface to 4600 m. The contour interval is 1^0 K.

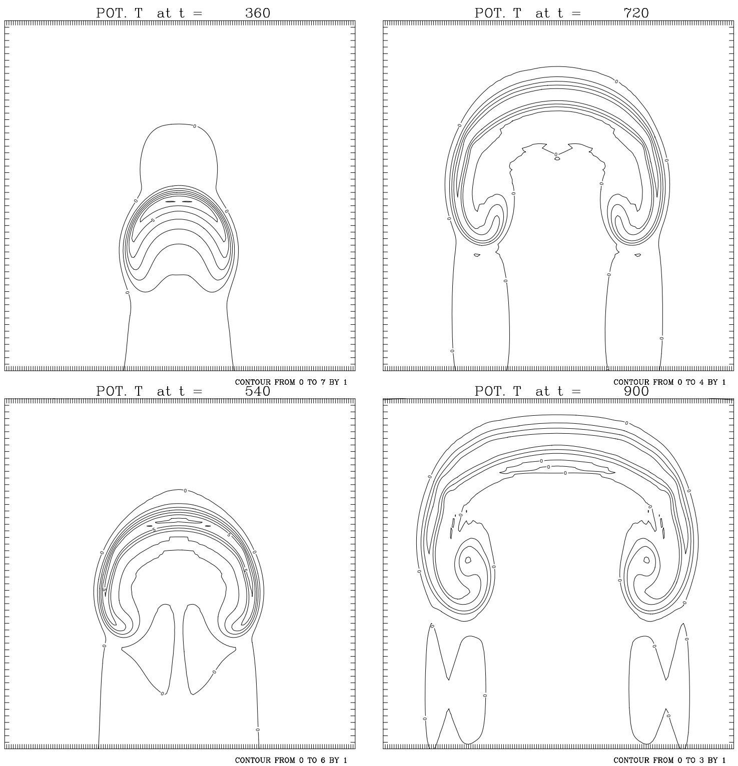

Potential temperature after 360 s, 540 s, 720 s and 900 s. The area shown extends 16 km along the x axis, and from 0 m to 13200 m along the z axis. The contour interval is 1^0K.

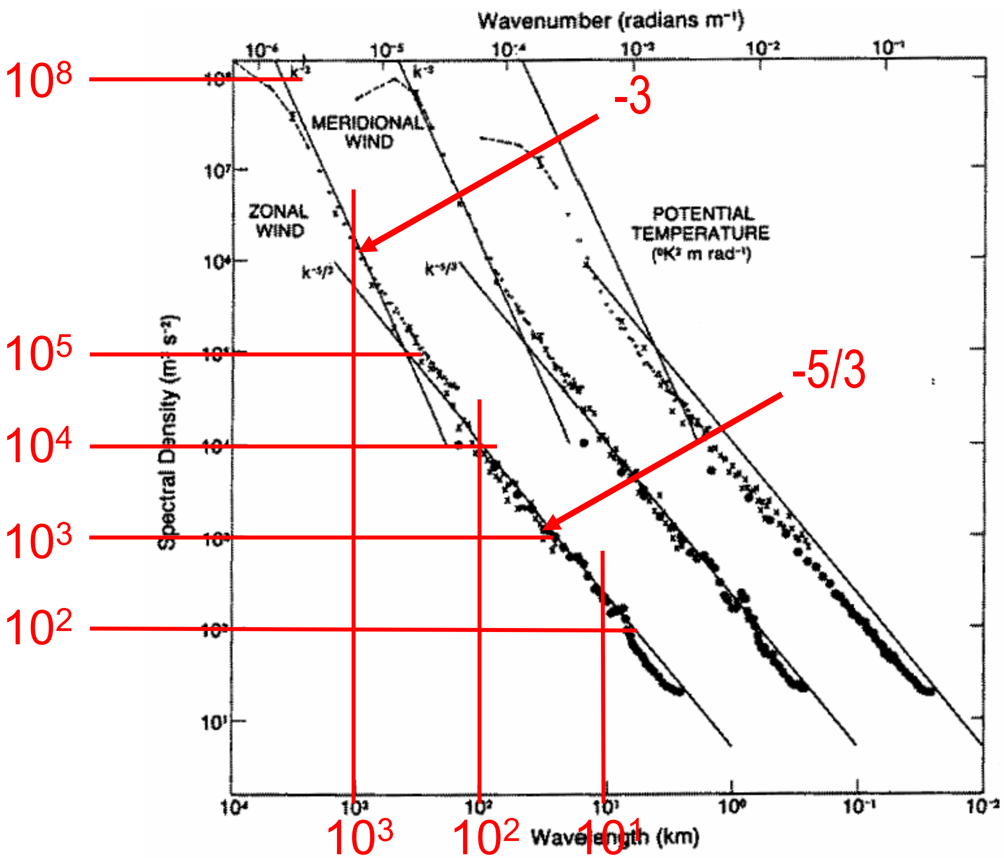

FIG. 1. Variance power spectra of wind and potential temperature near the tropopause from GASP aircraft data. The spectra for meridional wind and temperature are shifted one and two decades to the right, respectively; lines with slopes −3 and −5/3 are entered at the same relative coordinates for each variable for comparison. [Reproduced with permission from Nastrom and Gage (1985).]

- Nastrom-Gage (1985, JAS) 1D spectrum in upper troposphere and lower stratosphere from commercial aircraft measurements.
- No spectral gap.
- Transition at few hundred kilometers from –3 slope to –5/3 slope in the 10^2-10^3 km (mesoscale) range.
- Inertial range, 0.01-0.3 m s^{-1} in the –5/3 range, not to be confused with severe mesoscale phenomena!

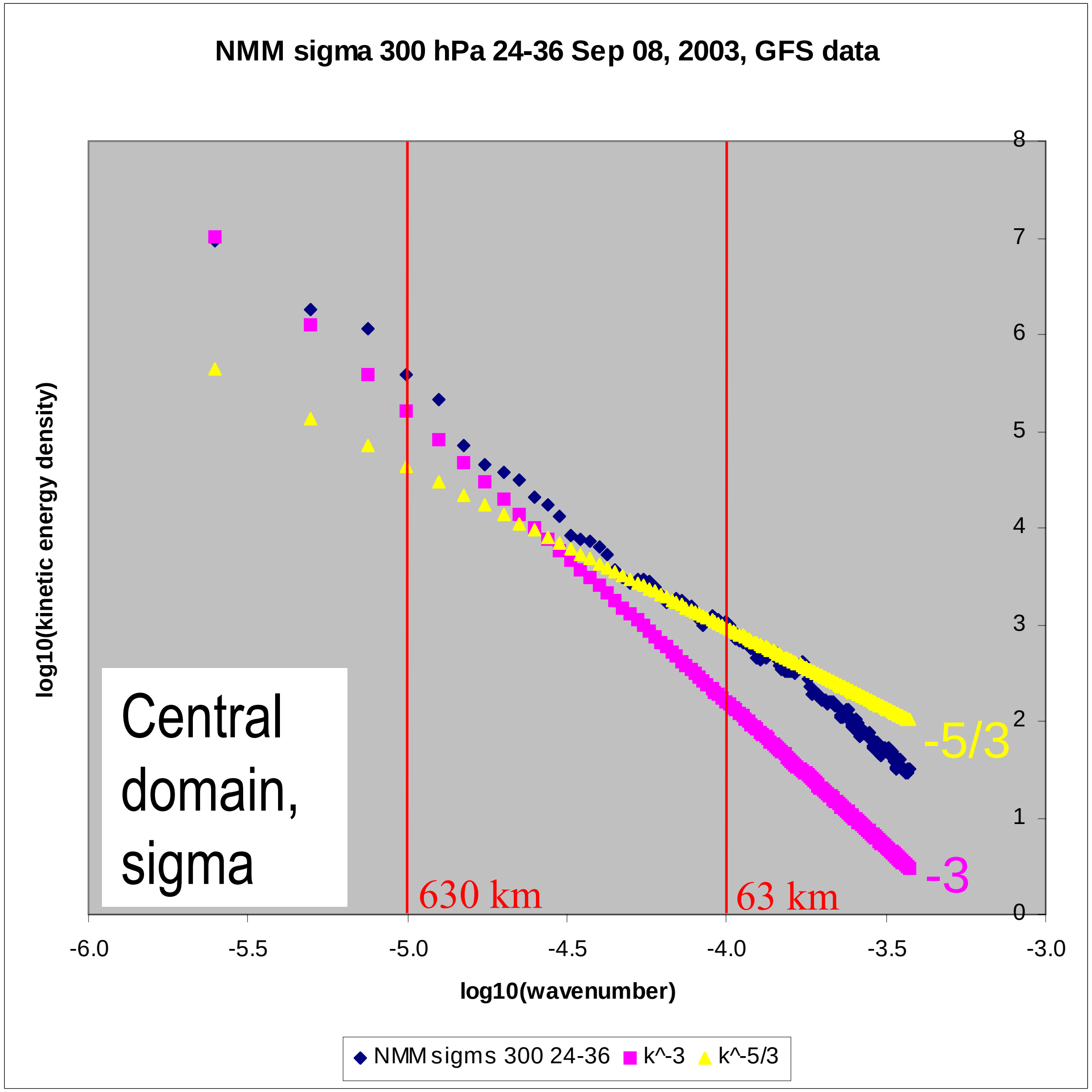
NMM sigma 300 hPa 24-36 Sep 08, 2003, GFS data
log10(kinetic energy density)
log10(wavenumber)
Central domain, sigma
630 km
63 km
-5/3
-3
-6.0
-5.5
-5.0
-4.5
-4.0
-3.5
-3.0
0
1
2
3
4
5
6
7
8
NMM sigms 300 24-36
k^-3
k^-5/3

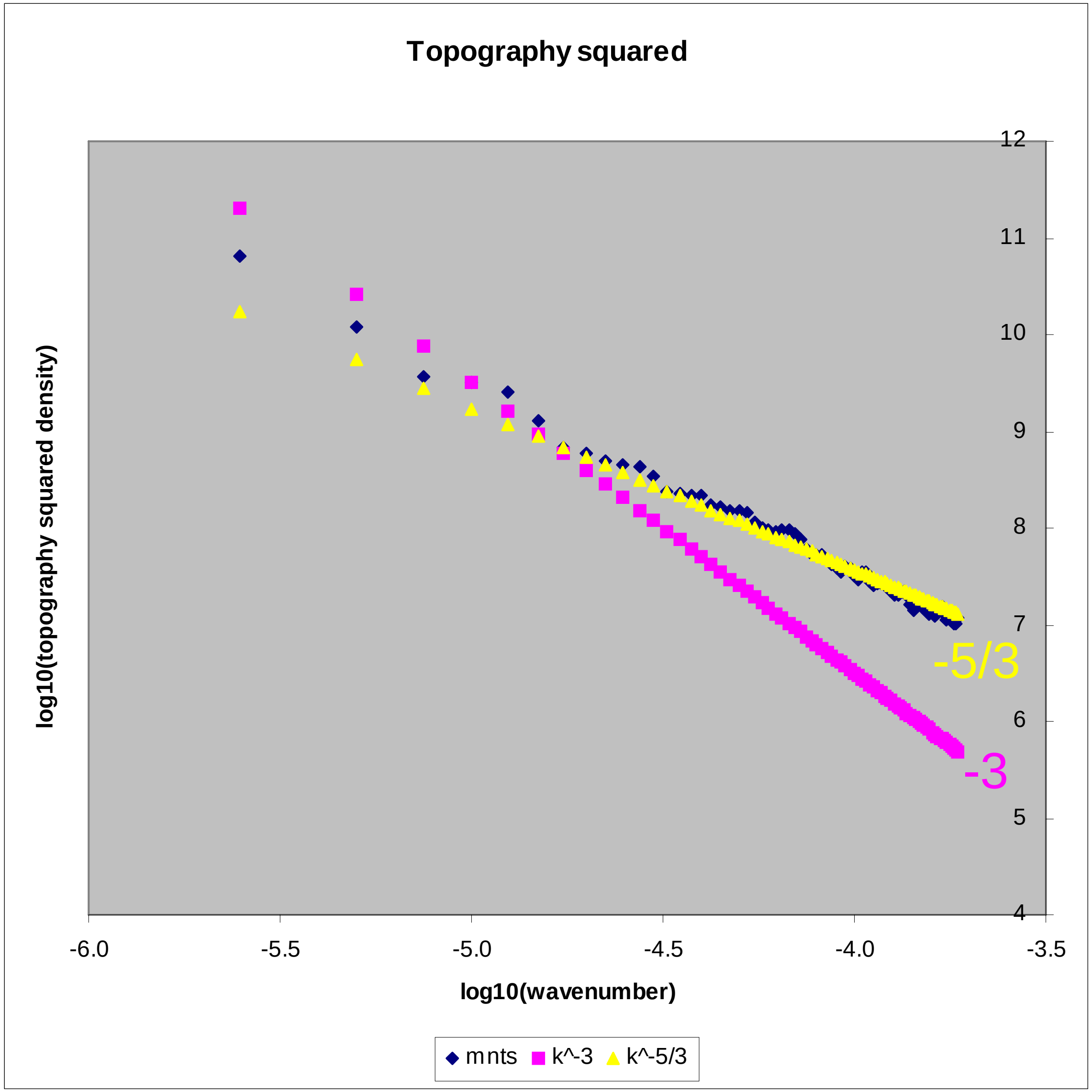

- Are the spectra forced by the sigma coordinate errors?

- Are the spectra just projections of the topography spectrum?

☞ We don't want the spectrum due to sigma errors!

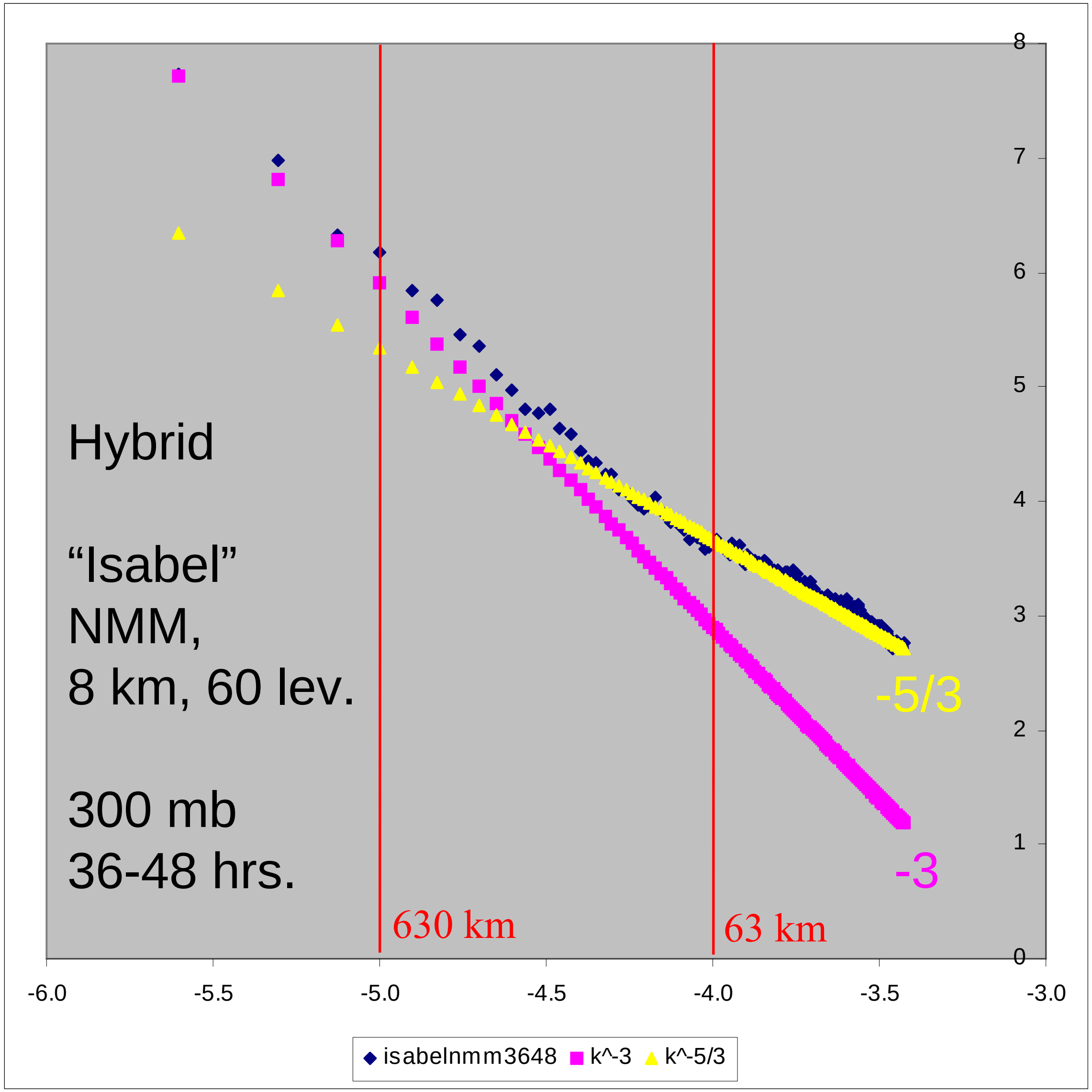
Hybrid
"Isabel"
NMM,
8 km, 60 lev.
300 mb
36-48 hrs.
630 km
63 km
-5/3
-3
0
1
2
3
4
5
6
7
8
-6.0
-5.5
-5.0
-4.5
-4.0
-3.5
-3.0
isabelnmm3648
k^-3
k^-5/3

Where is the small scale energy in the observed spectrum coming from?

Atlantic case, NMM-B, 15 km, 32 Levels, time loops

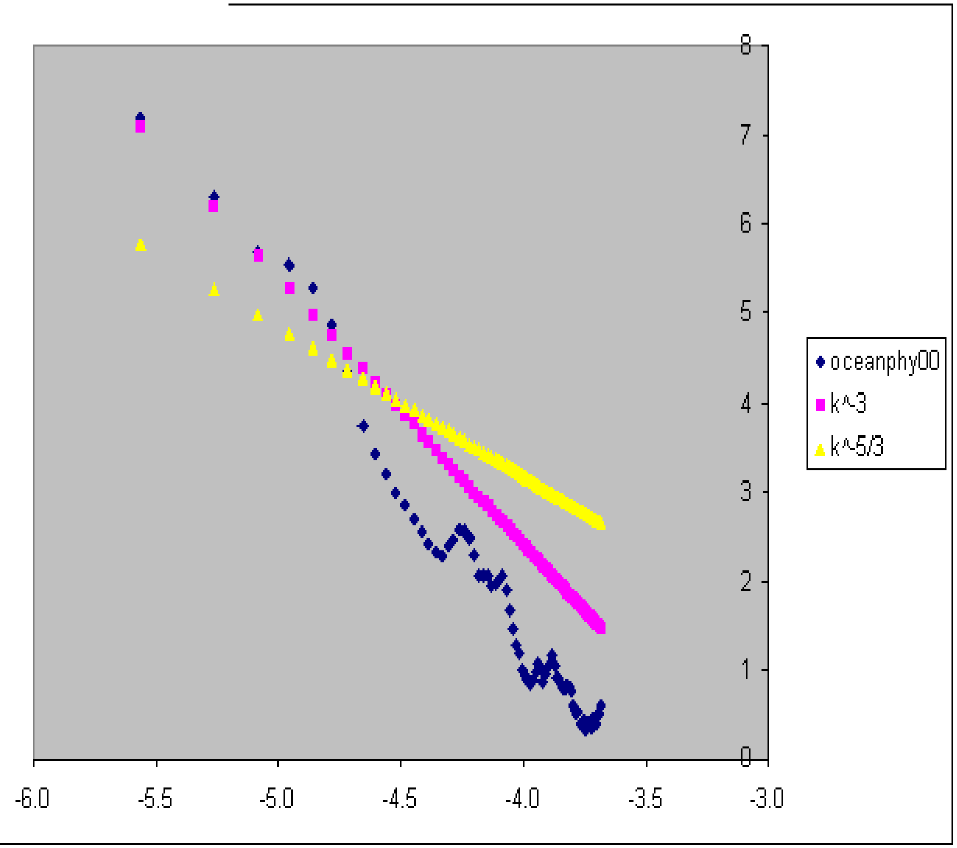

No Physics

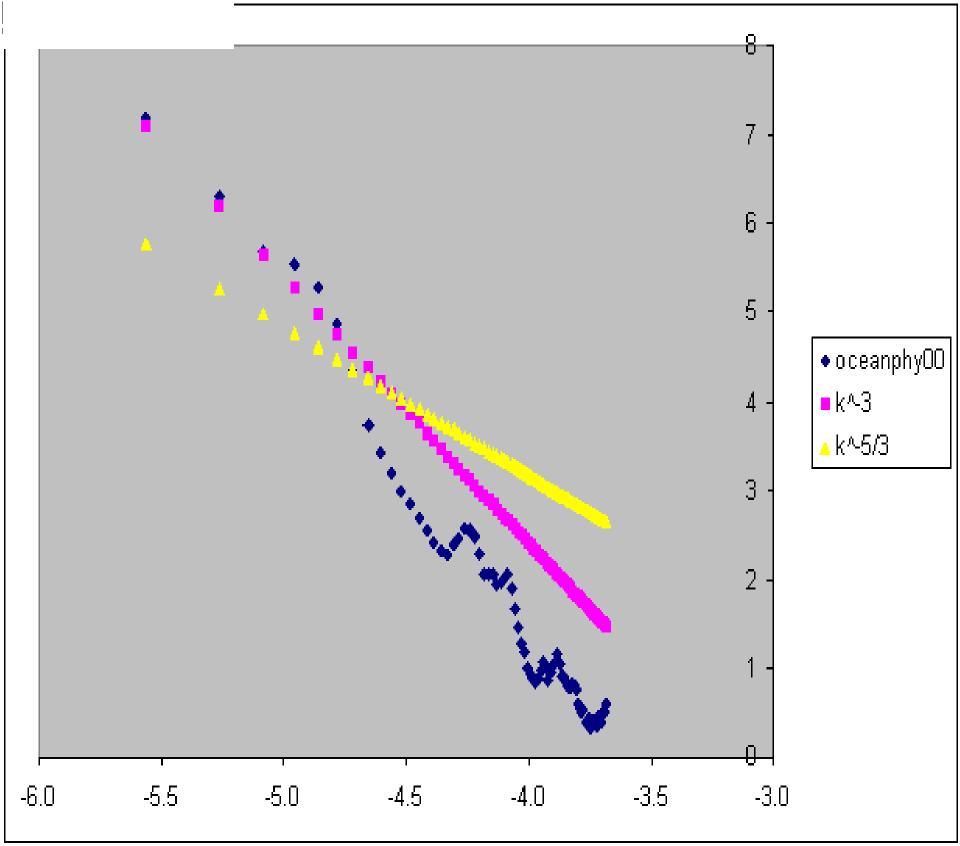

With Physics

Where is the small scale energy in the observed spectrum coming from?

Atlantic case, NMM-B, 15 km, 32 Levels, 36-48 hour average

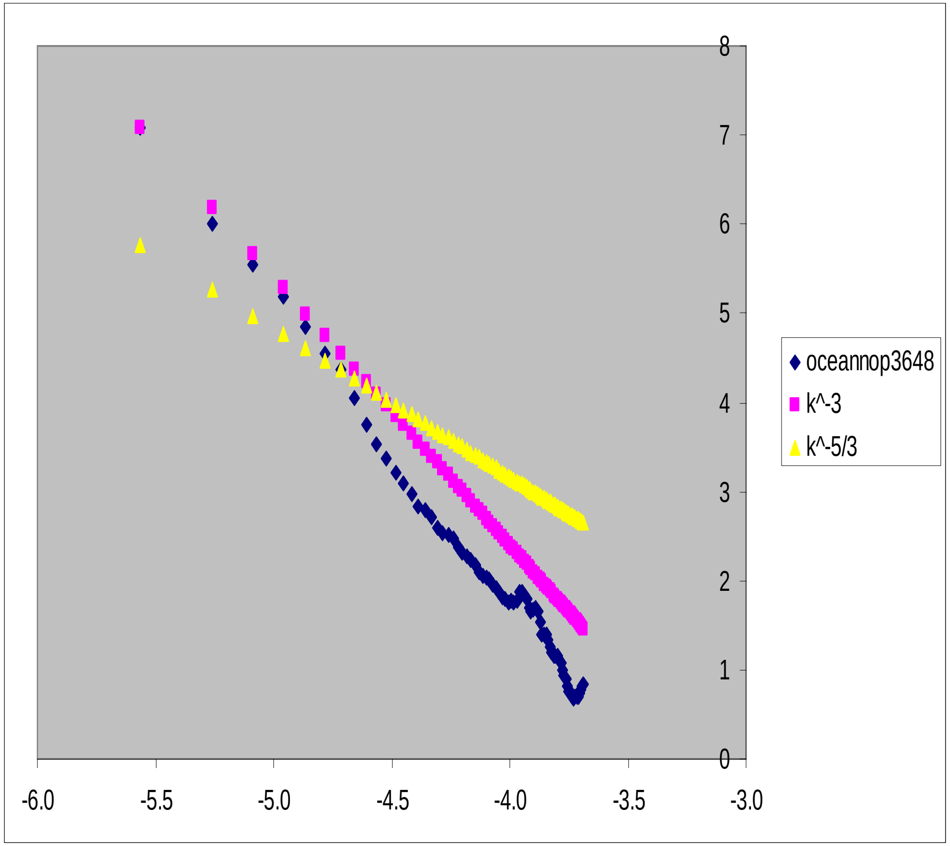

No Physics

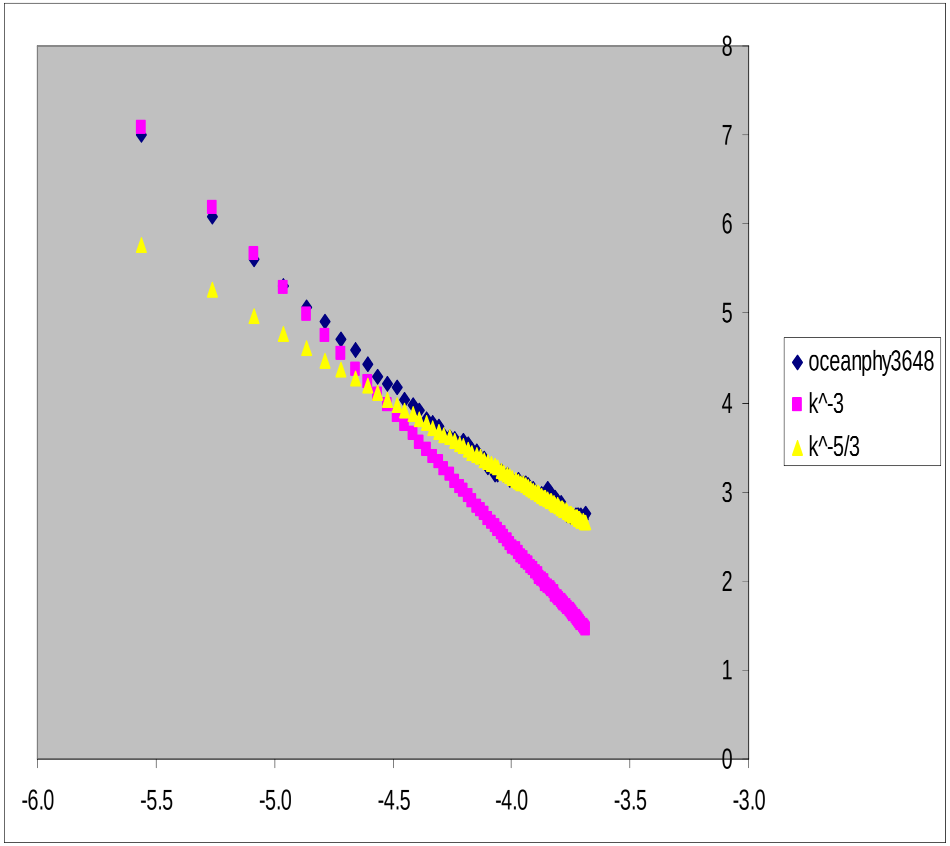

With Physics

Decaying 3D turbulence, Fort Sill storm, 05/20/77.

NMM-B,
Ferrier microphysics,
1km, 32 levels,
112km by 112km by 16.4km, double periodic.

Spectrum of w^2 at 700 hPa, loop

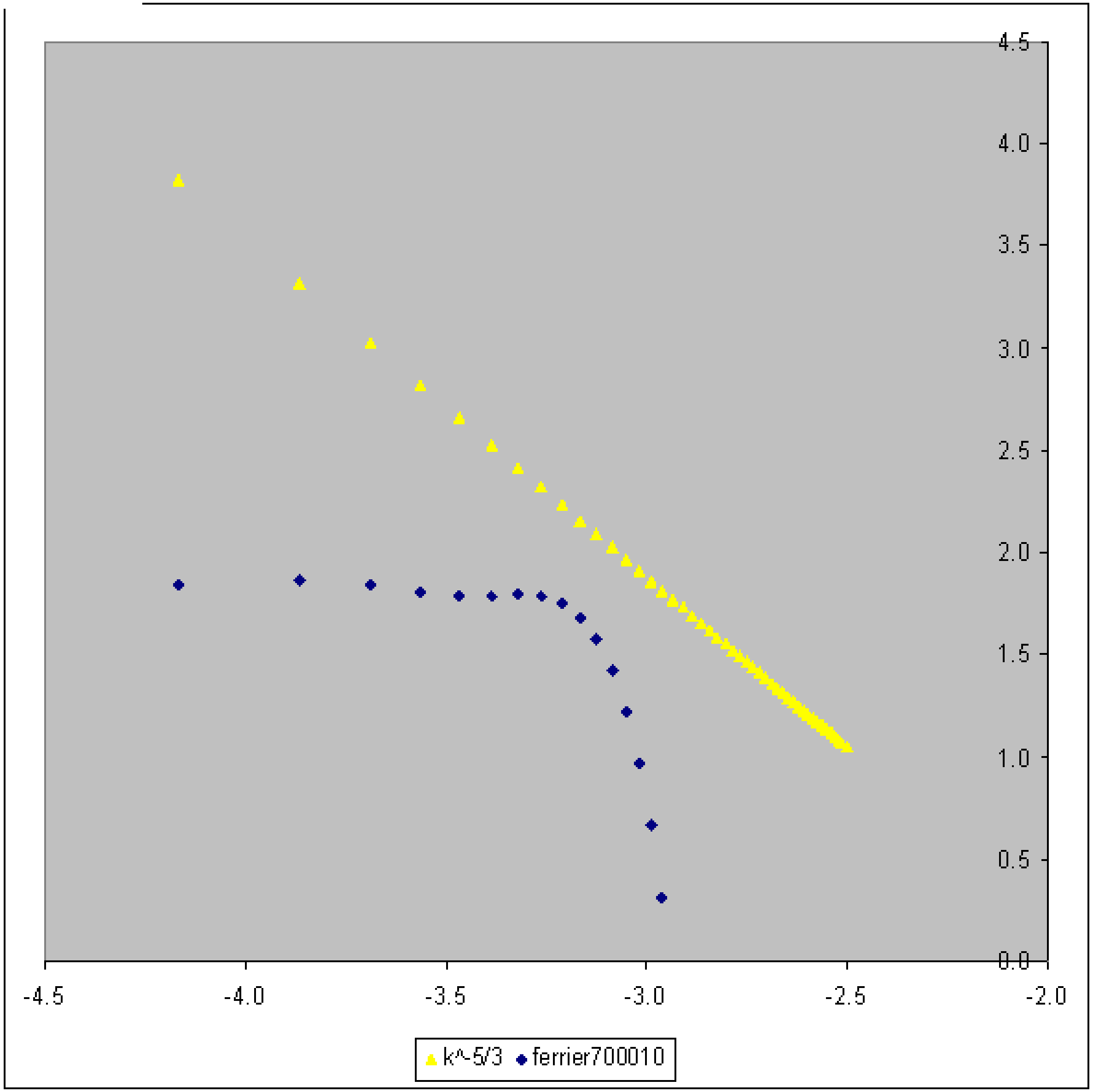

Decaying 3D turbulence, Fort Sill storm, 05/20/77.

NMM-B,
Ferrier microphysics, 1km, 32 levels, 112km by 112km by 16.4km, double periodic.

Spectrum of w^2 at 700 hPa, hours 3-4 average.

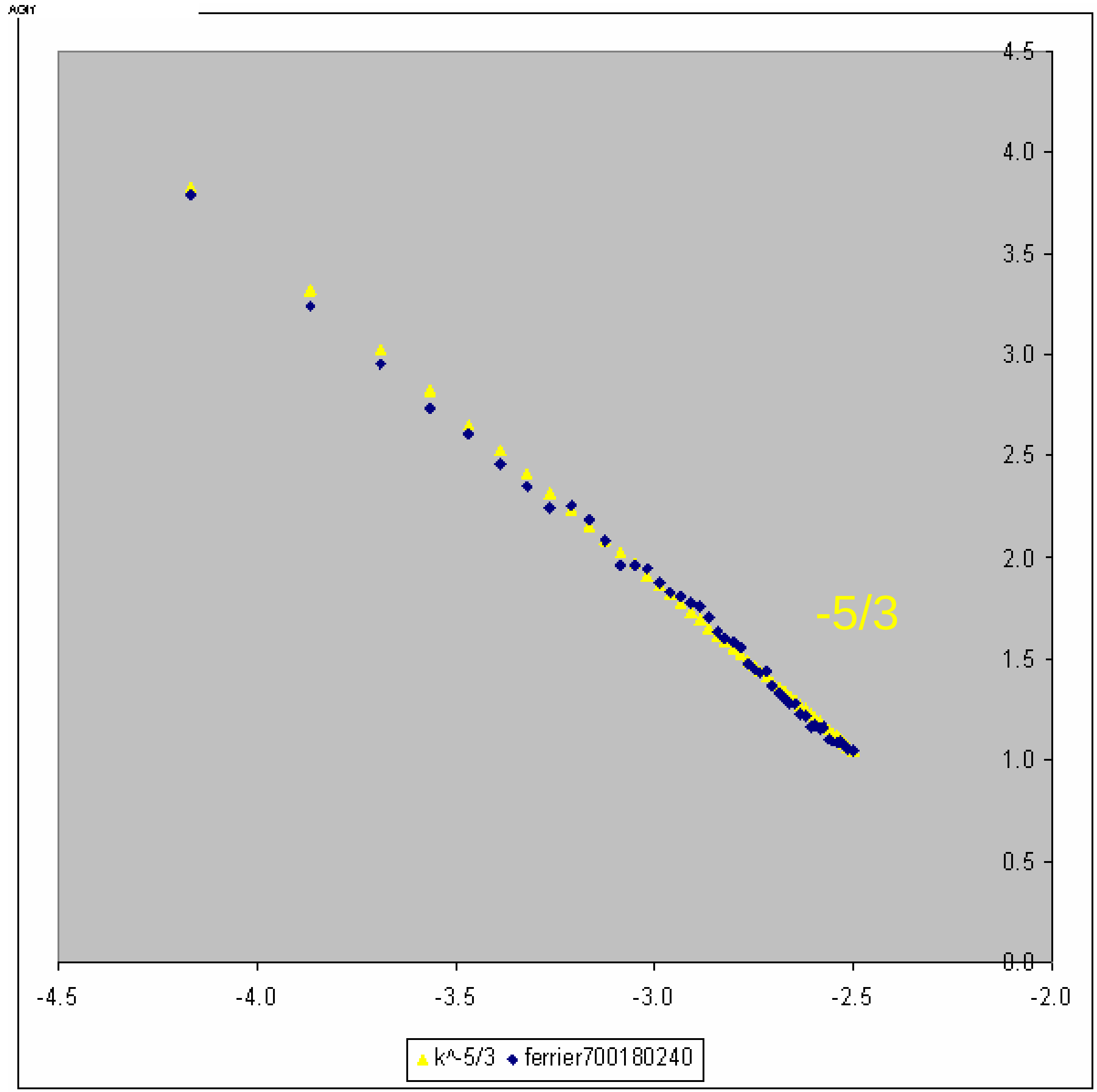

- Major spurious energy sources on small scales eliminated
- Excessive damping eliminated
- Excellent agreement with observed spectrum, provided physical energy sources on small scales
- Robust results across a range of horizontal resolutions and different grids

SLP NAMX 84H FCST VALID 12Z 05 FEB 2006

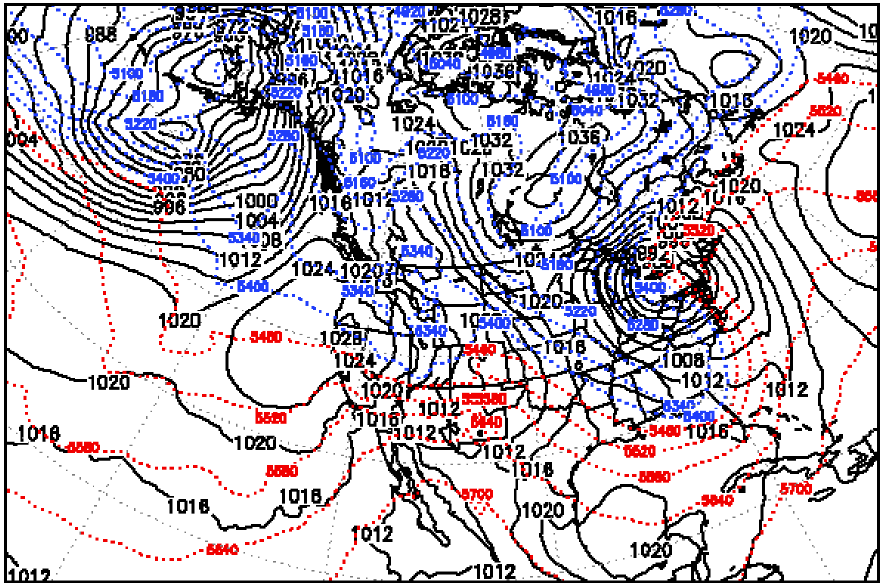

SLP GFS 00H FCST VALID 12Z 05 FEB 2006

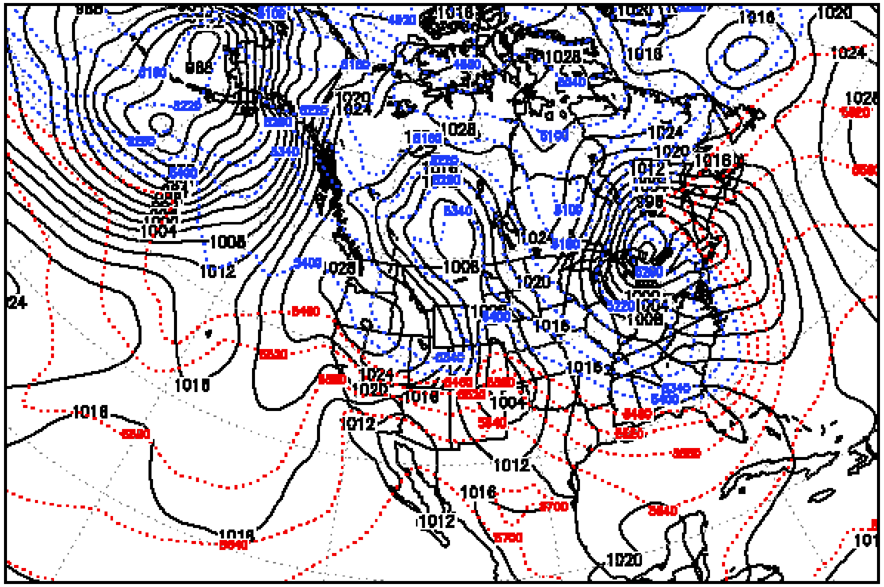

Verifying GFS analysis

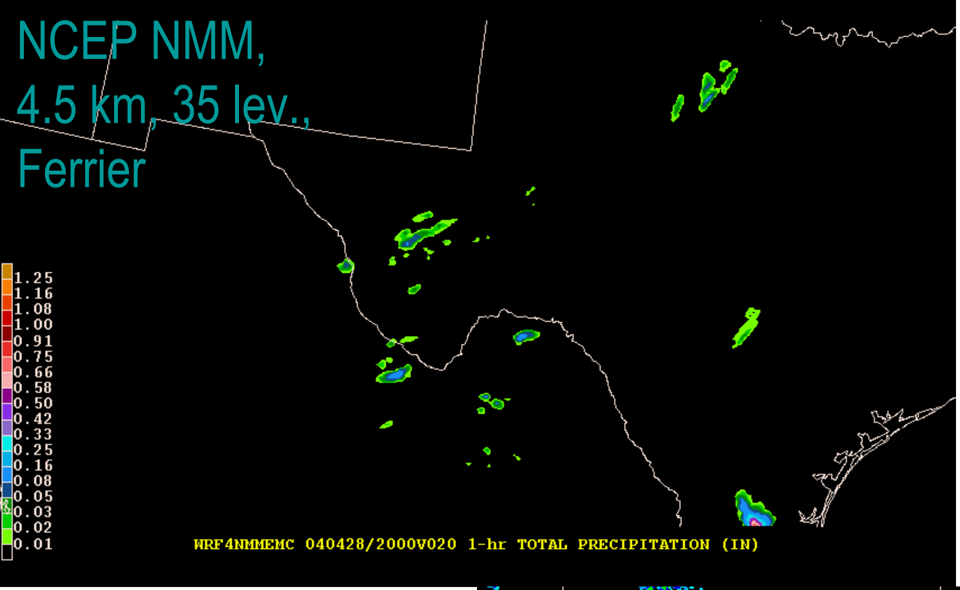

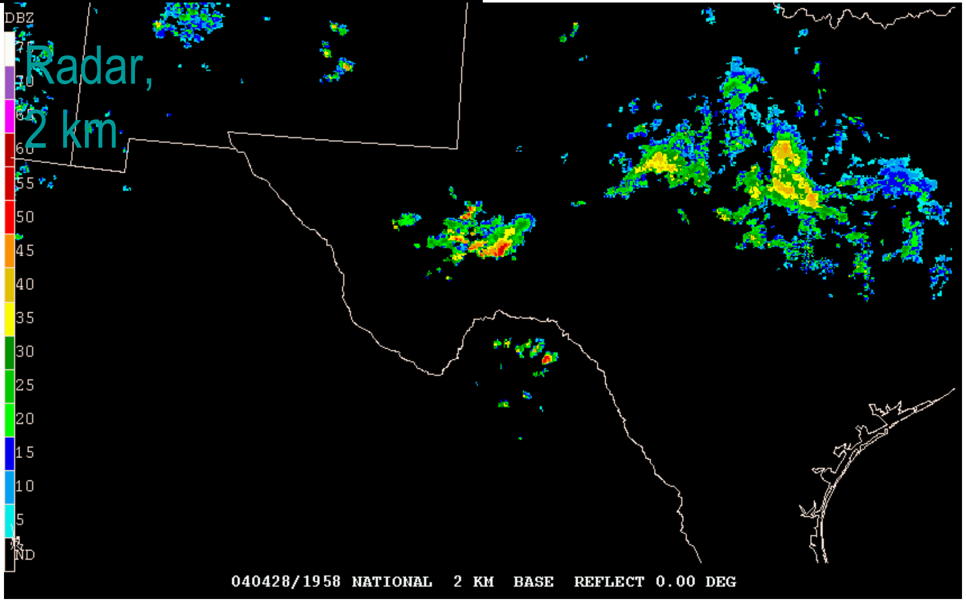

NSSL/SPC
2004 Spring
Program

04/04/28, 00Z
~ +24 hours

Courtesy:
Jack Kain,
Steve Weiss

☞ Development of the Hurricane WRF-NMM (HWRF) system (Naomi Surgi Program Leader)

- Joint effort of several institutions (EMC, FSU, GFDL, URI, ETL, HRD, Navy, ESSIC, RSMAS, PSU, USA).
- Large parent domain, multiple nest system.
- Specific physics.
- Coupling with ocean model.
- Planned to replace the GFDL model in operations in 2007.

- Two-way interactive nesting.
- Nest movement following the center of the storm (Gopalakrishnan et al., 2002, MWR).
- Parent domain about $60^0 \times 60^0$, about 27km resolution.
- Moving nest about $6^0 \times 6^0$, about 9km resolution.
- Currently GFS physics, constant SST.
- 55 minutes run time for 5 days forecasts on 72 processors.

AUG 25,2005 12Z:HURRICANE KATRINA - MOVING NEST FCST: 0

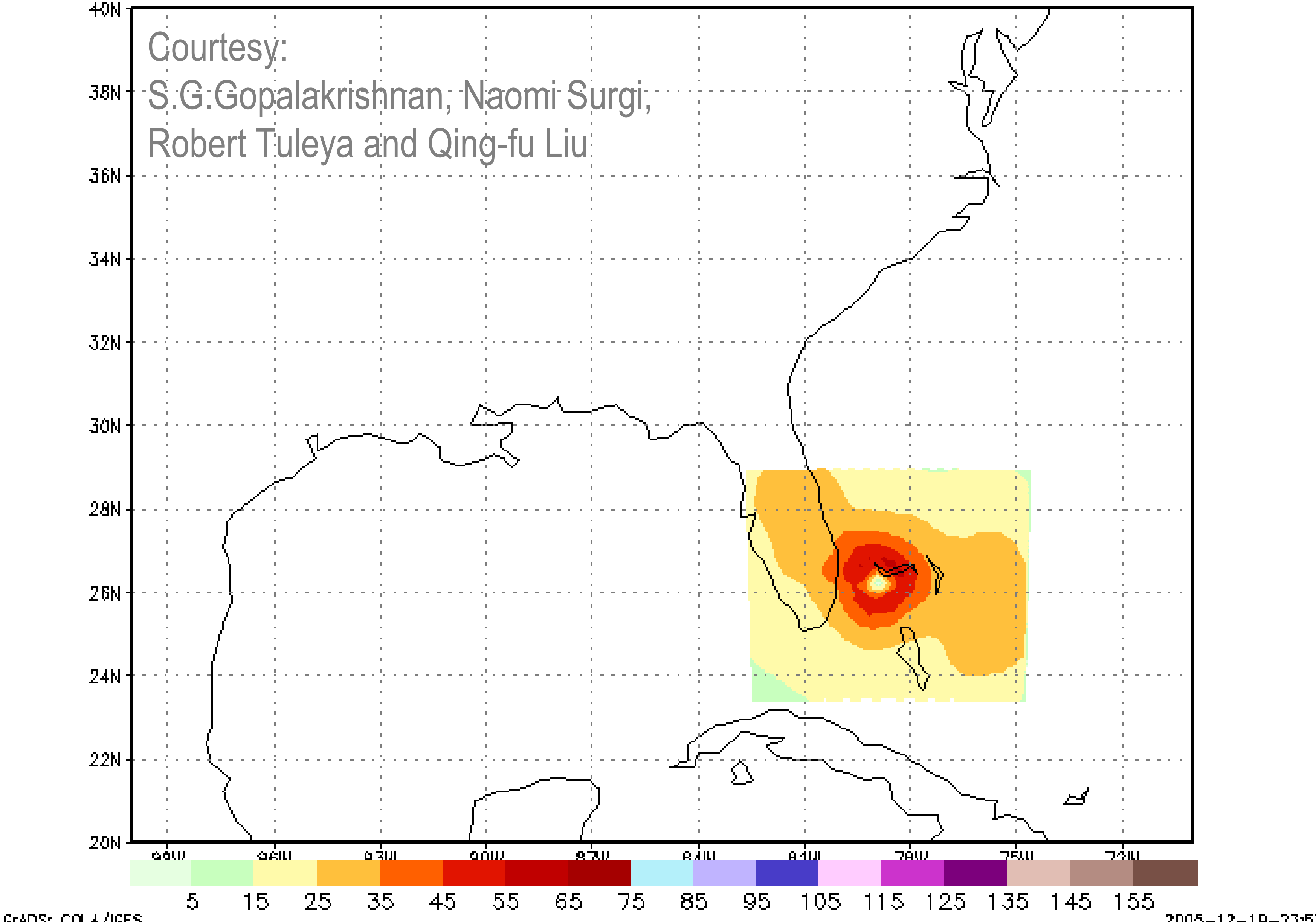

Five Day Forecasts with 2-Way Interactive Moving Nests

Courtesy:
S.G.Gopalakrishnan,
Naomi Surgi,
Robert Tuleya and
Qing-fu Liu

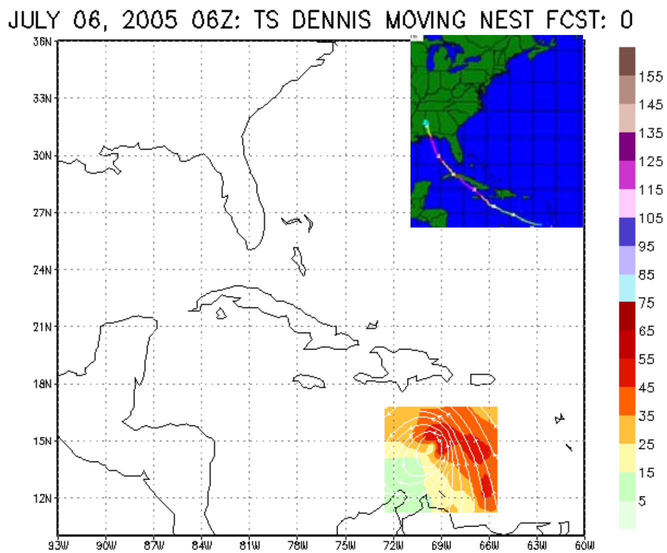

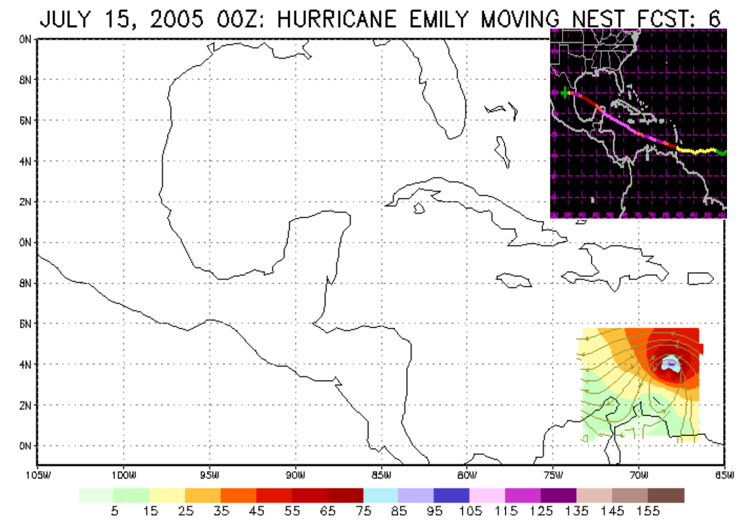

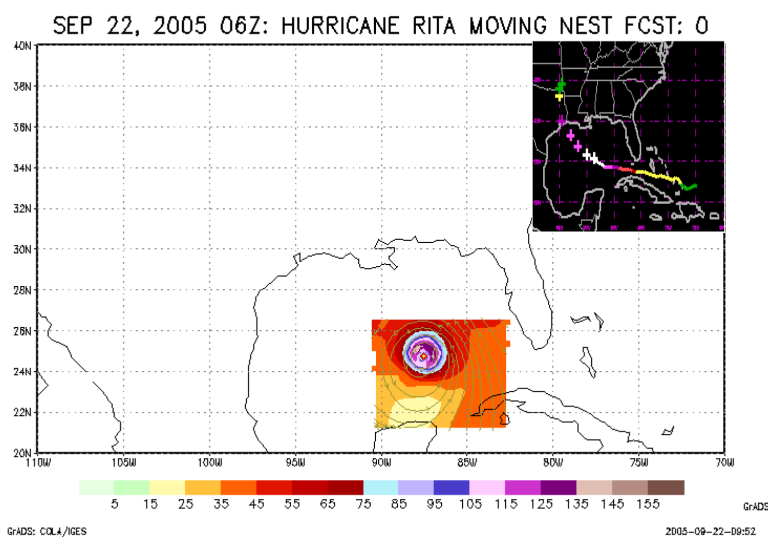

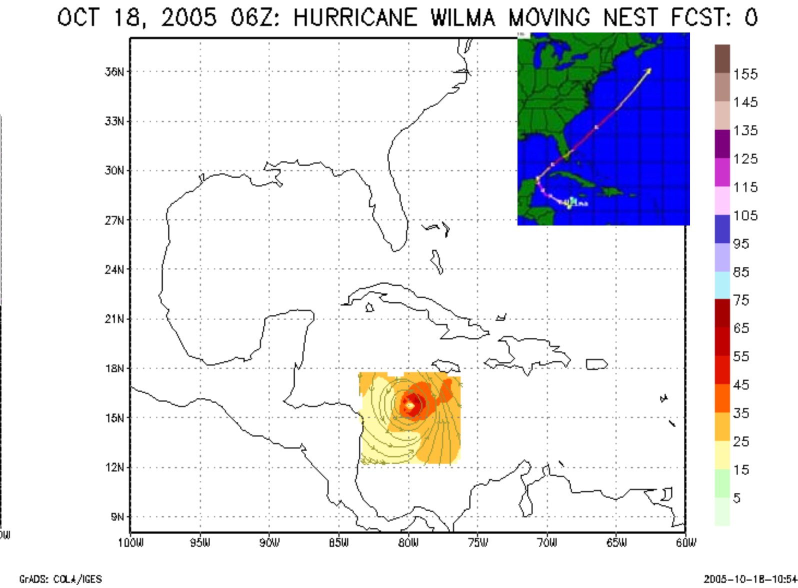

➢ Conclusions

- Robust, reliable, fast
- Atmospheric spectrum that is not due to computational noise
- NWP on near-cloud scales successful more frequently and with stronger signal than if only by chance
- Replaced the Eta as NAM at NCEP on June 20, 2006
- To become operational as hurricane WRF in 2007
- Operational and quasi-operational elsewhere